Noname manuscript No.
(will be inserted by the editor)

Spatial periodic orbits in the equilateral circular restricted four body problem

computer-assisted proofs of existence

Jaime Burgos-García · Jean-Philippe Lessard · J.D. Mireles James

Received: date / Accepted: date

Contents

Abstract We use validated numerical methods to prove the existence of spatial periodic orbits in the equilateral restricted four body problem. We study each of the vertical Lyapunov families (up to symmetry) in the triple Copenhagen problem, as well as some halo and axial families bifurcating from planar Lyapunov families. We consider the system with both equal and nonequal masses.

Our method is constructive and non-perturbative, being based on a-posteriori analysis of a certain nonlinear operator equation in the neighborhood of a suitable approximate solution. The approximation is via piecewise Chebyshev series with coefficients in a Banach space of rapidly decaying sequences. As byproduct of the proof we obtain useful quantitative information about the location and regularity of the solution.

Keywords Gravitational 4-body problem · spatial periodic orbits · Chebyshev spectral methods · computer-assisted existence proofs

The first author was supported by PRODEP grant UACOAH-PTC-416.
The third author was partially supported by NSF grant DMS-1700154 and by the Alfred P. Sloan Foundation grant G-2016-7320

Jaime Burgos-García
Facultad de Ciencias Físico Matemáticas, Universidad Autónoma de Coahuila. Unidad Campo redondo, Edificio A. Saltillo, Coahuila, 25020. México
E-mail: jburgos@uadec.edu.mx

Jean-Philippe Lessard
McGill University, Department of Mathematics and Statistics, 805 Sherbrooke West, Montreal, QC, H3A 0B9, Canada.
E-mail: jp.lessard@mcgill.ca

J.D. Mireles James
Florida Atlantic University, Department of Mathematical Sciences
E-mail: jmirelesjames@fau.edu

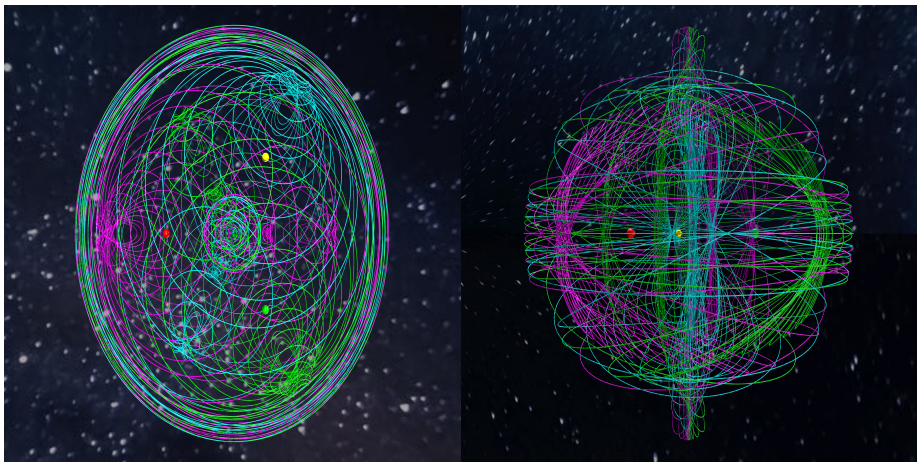

Fig. 1 Spatial periodic orbits in the triple Copenhagen problem: the figure illustrates 126 spatial periodic orbits in the equilateral restricted four body problem with equal masses. Computer assisted proofs of existence for these orbits – using the methods laid down in the present work – are discussed in Section 5. The triple Copenhagen problems has a $2\pi/3$ rotational symmetry, so that in this case we only have to prove $1/3$ of the orbits and obtain the rest by symmetry.

1 Introduction

A complete understanding of the gravitational $N-$body problem is among the oldest challenges in mathematical physics, with roots in the age of Newton. In the 19th century, Poincaré initiated the study of the circular restricted three body problem (CRTBP). In this simplified problem two massive bodies (called primaries) are constrained to a fixed periodic solution of the Kepler problem, and a massless particle moves in their gravitational field. This is one of the simplest N-body problems which is not integrable and which admits chaotic motions. A complete review of the literature for the CRTBP is beyond the scope of this work, and we direct the interested reader to the watershed studies of E. Strömgren [1], of M. Hénon [2], [3], and of R. Broucke [4]. We also refer to the books of Moser [5], of Szebehely [6], of Meyer and Hall [7], and of Belbruno [8]; and also to the lecture notes of Chenciner [9] for much more complete discussions.

The advent of space exploration in the Twentieth Century revitalized study of the CRTBP. Researchers developed new analytical and numerical techniques to find orbits for use in the design of space missions. One of the first works to study the possibility of using the R3BP to design space missions is found in the Ph.D. thesis of R.W. Farquhar [10]. He used some spatial periodic orbits in the CRTBP, the so–called *Halo orbits*, as hypothetical locations for communications relay stations in the Apollo missions. The first mission to actually use a spatial Halo orbit was the ISEE-3 satellite in 1978. Almost twenty years later the Solar and Heliospheric Observatory (SOHO) was the second mission using this kind of orbit in 1996. Again a complete review of past and future missions considering Halo orbits as trajectories is beyond the scope of this work, but it is worth mentioning that the James Webb Space Telescope – previously known

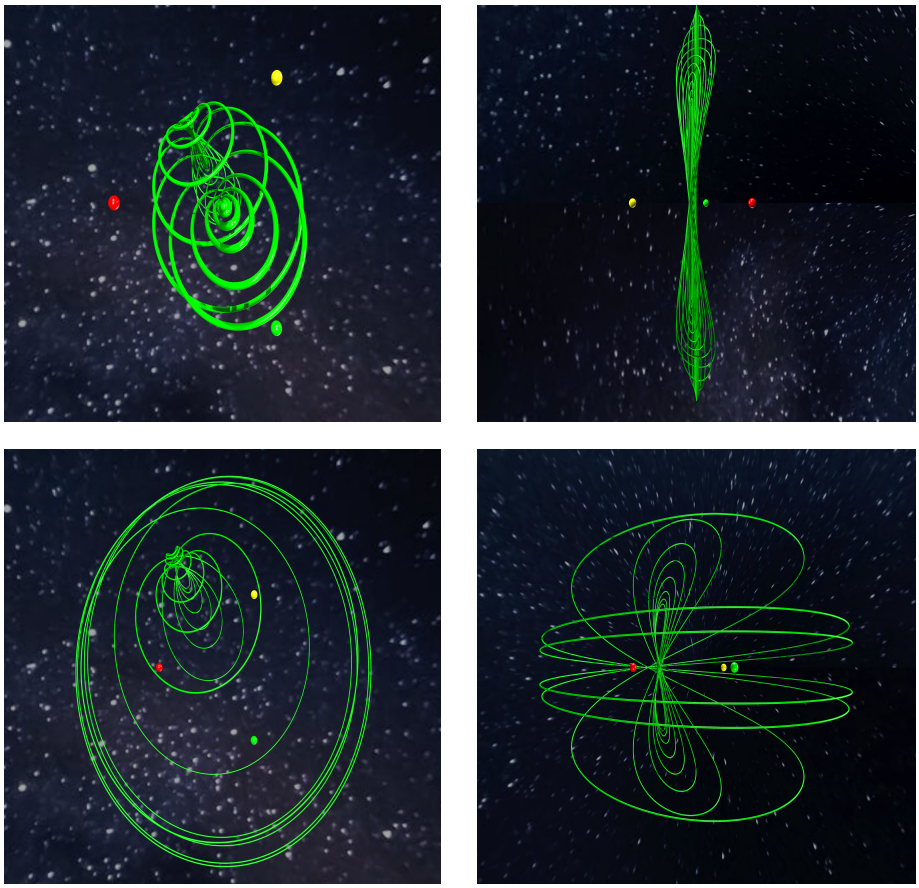

Fig. 2 Vertical Lyapunov families associated with libration points: the orbits illustrated in Figure 1 are obtained by numerical continuation from the vertical families associated with the 10 libration points of the triple Copenhagen problem. Our method of proof is based on a-posteriori analysis of numerical data, and applies to any of the orbits located during the continuation. This figure illustrates the vertical families associated with L_1 (top frames) and L_4 (bottom frames). See Section 2 for an overview of the libration points and their stability.

as Next Generation Space Telescope (NGST) – will be stationed on a Halo orbit near the libration point L_2 in the Sun–Earth system in 2019. We refer to the interested reader to [11] for further mission details.

Natural generalizations of the CRTBP consist in taking a special solution of the gravitational three body problem, and studying a massless particle moving in the resulting field. It is well known that the three body problem admits an explicit solution known as the Lagrangian central configuration. This consists of three massive (not necessarily equal) bodies arranged in an equilateral triangle configuration. Each body moves in a periodic orbit of the Kepler problem, either elliptical or – as in our case – circular. The resulting four body system is known as the equilateral circular restricted four body problem (CRFBP).

Let us briefly consider some motivation for studying the CRFBP. Astronomical observations reveal that Lagrangian central configurations are found in our own solar

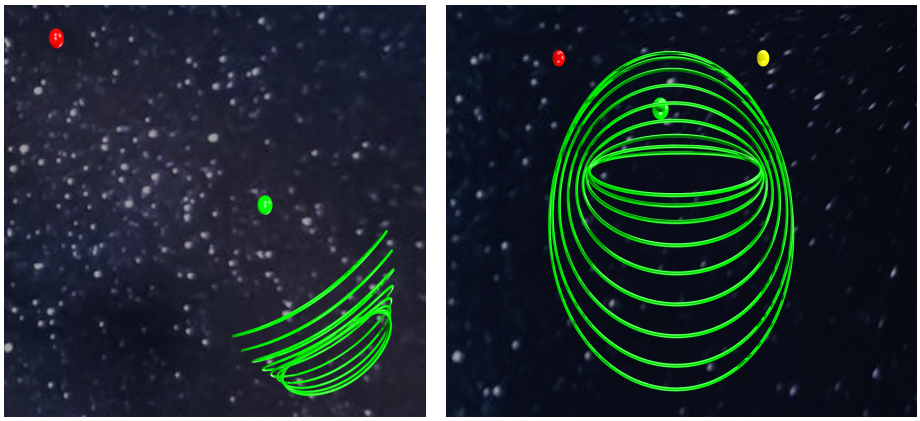

Fig. 3 Halo family in the equilateral restricted four body problem: spatial periodic orbits can appear as bifurcations from planar Lyapunov orbits. One such family is illustrated here for an equilateral restricted four body problem with non-equal masses/broken symmetry. We refer to these as halo orbits, in analogy with similar families found in the CRTBP – an observer sitting in the xy-plane sees these as "halos" around a primary body. We discuss existence proofs for these and several related families bifurcating from the plane in Section 5.

system. There are well known examples of asteroids that lie approximately in an equilateral configuration in the Sun-Jupiter system. Such asteroids have been classified into two groups, the so-called *Trojans* and *Greeks* which both lie on the orbit of Jupiter. Trojan asteroids have been detected recently in our solar system for the Mars-Sun and Neptune-Sun systems and even for the Earth-Sun system. We find equilateral triangle configurations also among Saturn and some of its moons, for example Saturn–Tethys–Telesto, Saturn–Tethys–Calypso or Saturn–Dione–Helene. Exploration of the Trojan asteroids was included with high priority in the *2013 Decadal Survey among the New Frontiers missions in the decade 2013-2022*.

In [12] the authors describe several observed extrasolar planetary systems (EPS) where they find a Sun-like star and a Jupiter-like gas giant orbiting the star. They compute the stability zones of hypothetical planets located approximately in an equilateral configuration formed by the star-gas giant-Trojan planet system. In other words, they consider hypothetical planets in a $1:1$ orbital resonance with the gas giant. They also consider some other relevant effects in their work, related to the habitability of the Trojan planet. For example they consider the age of the central star, the distance from it, climate considerations etcetera.

Mathematical investigations of the CRFBP appear as early as the work of Pedersen [13], [14]. A later study of Simó gave compelling numerical evidence for the conjecture that there are always eight, nine, or ten equilibrium solutions – depending on the mass ratios of the primary bodies [15]. The interested reader may want to consult also the study of Alvarez-Ramírez and Vidal [16] where tools from the qualitative theory of dynamical systems are used to explore the phase space of the spatial problem in detail.

A rigorous mathematical proof that Simó gave the correct equilibrium count for all masses values has recently been completed in a series of papers by Leandro and Barros

[17], [18], [19]. The proof uses Möbius transformations to put the problem into a form where the number of zeros is counted using rules of sign. From the point of view of the present discussion, it is important to mention that the proof is computer assisted.

The next simplest solutions of the CRFBP are periodic orbits, and these are studied in a number of works including Burgos, Delgado, and Bengochea [20], [21], [22], and Papadakis and Baltagiannis [23], [24], [25]. The paper [25] just cited is especially relevant to the present introduction, as the author studies some spatial families of periodic orbits in the CRFBP.

Inspired by the success of Leandro and Barros, we provide mathematically rigorous existence proofs for some spatial periodic orbits in the CRFBP. As in the works of Leandro and Barros, our method of proof is computer assisted. Of course the number of periodic orbits in a Hamiltonian system is typically uncountable, and we cannot hope to obtain precise counts as in the equilibrium case. Instead we focus on proving the existence of periodic orbits in certain prominent families like the vertical Lyapunov, Halo, and Axial solutions.

We present a method which can in principle be used to prove the existence of any non-degenerate periodic orbit for the CRFBP found using standard numerical methods. Here non-degeneracy amounts to assuming that the periodic orbit is isolated in the energy level set, and that it is not too close to a bifurcation. "Too close" involves implementation details like the number of digits of precision available in the representation of real numbers, the conditioning of certain matrices, and some local bounds on second derivatives.

Our arguments are based on a-posteriori analysis in infinite sequence spaces of Chebyshev series coefficients. The method is constructive, works for parameter values far from any symmetric or perturbative special cases, and provides useful bi-product such as precise bounds on the location of the orbits, bounds on derivatives, bounds on the domain of analyticity, and decay rates for the Chebyshev series coefficients of the periodic orbit. Some periodic orbits whose existence is proved using our methods are illustrated in Figures 1, 2, and 3. More results are discussed in Section 5.

Our computer-assisted analysis builds on the earlier work of Ransford, Hungria, Lessard and Mireles-James [26], [27], incorporating new developments due to Sheombarsing and van den Berg [28] (see Section 4), and Lessard [29] (see Remark 3). Indeed we defer to these references for many of the technical details, and focus our attention instead on adapting these methods to the CRFBP and on the results so obtained.

The remainder of the paper is organized as follows. In Section 2 we review some background material pertaining to the a-posteriori analysis. We also discuss briefly the rich literature on computer-assisted proof in celestial mechanics. In Section 3 we discuss a procedure which transforms our problem to polynomial, and introduce appropriate phase conditions for periodic orbits in the transformed problem. In Section 4, we introduce the Chebyshev operator equation of the form $F(x) = 0$ whose solutions correspond to periodic orbits of the CRFBP. Section 5 is devoted to results, where we prove existence of periodic orbits in the CRFBP by showing existence of solutions of $F = 0$ using a rigorous computer-assisted a-posteriori analysis.

2 Background

2.1 Equations of motion for the equilateral circular restricted four body problem

We consider the motion of an infinitesimal particle, moving in the gravitational field of three massive bodies – the primaries – themselves moving in an equilateral triangular configuration of Lagrange. The equations of motion in a rotating frame are

$$\dot{\mathbf{x}} = f(\mathbf{x}),$$

where $\mathbf{x} \stackrel{\text{def}}{=} (x, \dot{x}, y, \dot{y}, z, \dot{z})$ and with the vector field given by

$$f(\mathbf{x}) \stackrel{\text{def}}{=} \begin{pmatrix} \dot{x} \\ 2\dot{y} + \Omega_x(x,y,z) \\ \dot{y} \\ -2\dot{x} + \Omega_y(x,y,z) \\ \dot{z} \\ \Omega_z(x,y,z) \end{pmatrix}. \tag{1}$$

Here

$$\Omega = \Omega(x, y, z, m_1, m_2, m_3) \stackrel{\text{def}}{=} \frac{1}{2}(x^2 + y^2) + \frac{m_1}{r_1} + \frac{m_2}{r_2} + \frac{m_3}{r_3}$$

is the effective potential, where $r_i \stackrel{\text{def}}{=} \sqrt{(x - x_i)^2 + (y - y_i)^2 + z^2}$, for $i = 1, 2, 3$. The general expressions for the coordinates of the primaries in terms of the masses of the three point masses are given by

$$x_1 \stackrel{\text{def}}{=} \frac{-|K|\sqrt{m_2^2 + m_2 m_3 + m_3^2}}{K}, \qquad y_1 \stackrel{\text{def}}{=} 0,$$

$$x_2 \stackrel{\text{def}}{=} \frac{|K|\left[(m_2 - m_3)m_3 + m_1(2m_2 + m_3)\right]}{2K\sqrt{m_2^2 + m_2 m_3 + m_3^2}} \qquad y_2 \stackrel{\text{def}}{=} \frac{-\sqrt{3}m_3}{2m_2^{3/2}}\sqrt{\frac{m_2^3}{m_2^2 + m_2 m_3 + m_3^2}}$$

$$x_3 \stackrel{\text{def}}{=} \frac{|K|}{2\sqrt{m_2^2 + m_2 m_3 + m_3^2}}, \qquad y_3 \stackrel{\text{def}}{=} \frac{\sqrt{3}}{2\sqrt{m_2}}\sqrt{\frac{m_2^3}{m_2^2 + m_2 m_3 + m_3^2}}$$

where $K \stackrel{\text{def}}{=} m_2(m_3 - m_2) + m_1(m_2 + 2m_3)$ and the masses are normalized so that

$$m_1 + m_2 + m_3 = 1.$$

We write

$$p_1 = (x_1, y_1), \qquad p_2 = (x_2, y_2), \qquad \text{and} \qquad p_3 = (x_3, y_3)$$

to denote the locations in the plane of the primary bodies.

The equations of motion have the well known first integral (the so-called *Jacobi constant*) given by

$$C = -(\dot{x}^2 + \dot{y}^2 + \dot{z}^2) + 2\Omega.$$

The constant C is related to the total energy of the system by means of the relation $E = -C/2$. It should be noted that when $m_3 = 0$ and $m_2 \stackrel{\text{def}}{=} \mu$ we recover the coordinates of the restricted three body problem:

$$\begin{aligned} (x_1, y_1, z_1) &= (-\mu, 0, 0), \\ (x_2, y_2, z_2) &= (1 - \mu, 0, 0), \\ (x_3, y_3, z_3) &= (1/2 - \mu, \sqrt{3}/2, 0), \end{aligned}$$

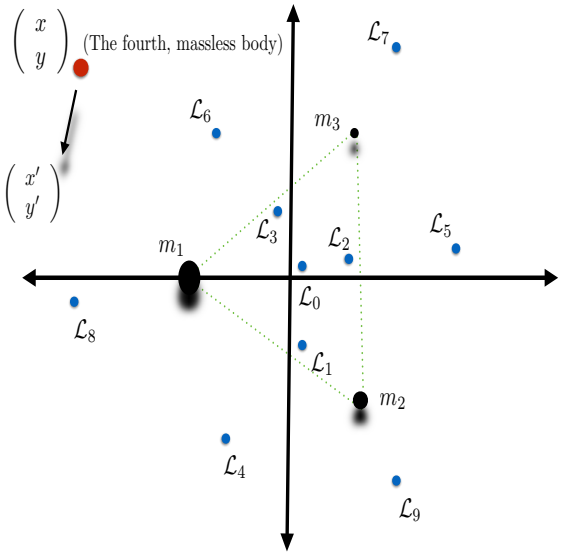

Fig. 4 The Circular Restricted Four Body Problem: the primaries with masses $0 < m_3 \leq m_2 \leq m_1$ move in a central equilateral triangle configuration of Lagrange. After changing to a co-rotating coordinate frame, we study the dynamics of a fourth and massless particle moving in the gravitational field of the primaries. The equations of motion for the massless particle are given by Equation (1). For typical mass ratios the problem has always 8, 9, or 10 relative equilibria (or libration points) depending on the mass ratio. The relative equilibria are denoted here by $\mathcal{L}_j$ for $0 \leq j \leq 9$.

where the position of the 'phantom' mass m_3 coincides with the equilibrium point L_4 of the R3BP associated to the masses m_1 and m_2.

The relative equilibria – or *libration points* – of the system are given by the critical points of the effective potential Ω. That is, they satisfy the equations $\Omega_x = 0$, $\Omega_y = 0$ and $\Omega_z = 0$. A straightforward computation shows that the partial derivative Ω_z satisfies

$$\Omega_z = -z \sum_{i=1}^{3} \frac{m_i}{r_i^3},$$

with $r_i = \sqrt{(x - x_i)^2 + (y - y_i)^2 + z^2}$ for $i = 1, 2, 3$, and as a consequence all equilibria are coplanar (i.e. $\Omega_z = 0$ implies that $z = 0$). As mentioned in the introduction, there are 8, 9, or 10 equilibria depending on the mass ratios.

It is not difficult to see that when we have two equal masses, say $m_2 = m_3$, the partial derivatives of the effective potential for the planar case satisfy the following properties

$$\Omega_x(x, -y) = \Omega_x(x, y),$$
$$\Omega_y(x, -y) = -\Omega_x(x, y).$$

As a consequence, the equations of motion (1) are invariant under the transformations $x \to x$, $y \to -y$, $\dot{x} \to -\dot{x}$, $\dot{y} \to \dot{y}$, $\ddot{x} \to \ddot{x}$, $\ddot{y} \to -\ddot{y}$ therefore, we have recovered the well known symmetry with respect to the x-axis for the restricted three body problem.

However, for the equal masses case we have an additional and useful symmetry which states that if $z(t) = x(t) + iy(t)$ is a solution of the system (in complex notation) then $e^{\frac{2\pi}{3}i} z(t)$ is also a solution of the system. In other words, we have a symmetry with respect to the lines that join the center of the triangle with the three primaries, see [30] for further details. A useful consequence of this symmetry with respect to the local dynamics around the equilibrium points is that it will be enough to study the equilibrium points on the x-axis. The information of such study can be extended to the remaining equilibrium points by means of this symmetry. Moreover, as this property can be applied to study the periodic orbits around the primaries, it will enough to study the dynamics around the primary on the x-axis.

2.2 Overview of methods and results

In the search for periodic orbits a natural starting point is the so-called vertical Lyapunov families. These are one parameter families of spatial periodic orbits near a libration point of saddle × saddle × center or saddle × center × center stability. For these we compute a high order approximation of the center manifold using the approach of Jorba and Farrés [31], which provides good starting points for the vertical Lyapunov families. We then apply a classical numerical continuation (e.g. see [32]). Since our continuation approach is based on Newton's method, we must have local isolation of the solutions. To get the isolation, we introduce *unfolding parameters* as introduced by Muñoz-Almaraz, Freire, Galán, Doedel, and Vanderbauwhede [33]. We apply our method of proof to some of the orbits located using the continuation scheme.

Another mechanism giving rise to spatial periodic orbits is discussed in the work of M. Hénon [34], and starts by considering a planar family of periodic orbits. He shows that computing the so-called vertical stability index (denoted as a_v) of a planar periodic orbit provides information about whether a planar periodic orbit belongs at the same time to a family of $3D$ (spatial) periodic orbits. The conclusions of that work suggest that the so-called vertical critical orbits, when $|a_v| = 1$, can be considered as members of $3D$ families of periodic orbits. When we find planar Lyapunov orbits for which $|a_v| = 1$, we will find spatial families of periodic orbits after the bifurcation. This mechanism produces the so-called halo and axial orbits families (as well as others). Once again numerical continuation can be applied to any such orbit, and we apply our method of proof to some periodic orbits located this way.

We now outline the main idea behind the computer-assisted proofs carried in the present work. Let $\Omega \subset \mathbb{R}^N$ be an open set and $f\colon \Omega \to \mathbb{R}^N$ be a real analytic vector field. The main objects of study in this paper are periodic solutions of the differential equation $\dot{\mathbf{x}} = f(\mathbf{x})$, that is solutions $\mathbf{x}\colon [0, T] \to \mathbb{R}^N$ with $\mathbf{x}(t+T) = \mathbf{x}(t)$ for all $t \in \mathbb{R}$. Following closely the approach of Sheombarsing and van den Berg [28], we expand the solution in the basis of Chebyshev series on multiple time domains, and we solve for the Chebyshev coefficients. We endow the space of unknown coefficients with a Banach space structure, and are left with the problem of finding a zero of a smooth nonlinear map between Banach spaces. Truncating to a finite number of modes we compute an approximate solution using Newton's method. Finally we make a posteriori arguments which allow use to conclude that there is a true solution of the problem near our numerical approximation. The a-posteriori analysis used in the present work follows the approach developed in [26, 28].

Using the methods sketched above, we are able to prove the existence of a number of in and out of plane periodic orbits for the CRFBP.

Remark 1 (Automatic differentiation) The analysis outlined above is based on formal series manipulations, and is especially straightforward when the vector field f is polynomial. However in the present work we consider the CRFBP, whose nonlinearities involve rational denominators originating from the inverse square law of universal gravitation. To circumvent this difficulty, our approach builds on the techniques of automatic differentiation for Fourier series developed in [27], and we convert the four body vector field into a polynomial system – albeit in a higher dimensional phase space. The idea, which we discuss in details in Section 3, is to append additional polynomial differential equations related to the rational nonlinearities. By carefully adding new variables (sometimes called unfolding parameters) to the system (which balance certain scalar constraint equations) we obtain a system of polynomial equations which is equivalent to the original system, in the sense that periodic solutions of one are periodic solutions of the other. We note that in [27] additional variable were avoided by exploiting the symmetries of the restricted three body problem.

2.3 Computer-assisted proofs in celestial mechanics

In this section we provide a brief overview of the literature on computational proofs for N-body problems, with a particular emphasis on results pertaining to periodic solutions. A thorough and general review of the literature on computer-assisted proofs in analysis is beyond the scope of the present work, and the interested reader will find extensive scholarly discussion in the book of Tucker [35], the memoire [36], and also the review articles [37,38]. The reader is warned also that the discussion below follows a kind of dynamical progression, and is not at all in chronological order.

Regular motions include equilibrium, periodic, and quasi-periodic solutions of the equations of motion. For example, while it is often possible to study equilibrium solutions and their stability for Hamiltonian systems "by hand" (or with the aid of computer algebra systems), it can be much more difficult to understand the nonlinear stability problem. We refer to the mathematically rigorous, computer-assisted studies of center manifolds [39] and strong stable/unstable manifolds [40] for the circular restricted three body problem, as well as to the work of [41] on the dynamics of complex saddles in the CRFBP.

Much effort has gone into developing techniques for computer-assisted proofs of periodic orbits for differential equations in general, and for celestial mechanics problems in particular. See for example the studies of [27,42] on periodic orbits for the three body and the planar restricted three body problem, as well as the computer-assisted proof of the existence of choreography orbits for N-bodies with $3 \leq N \leq 8$ [43]. The present work provides computer-assisted proofs of spatial orbits in the circular restricted four body problem. The work of [44] proves the existence of one parameter families of Halo orbits in the restrected three body problem and studies their bifurcations via mathematically rigorous computations.

Computer-assisted proofs of invariant tori in realistic celestial systems are both difficult and technical, and can be found in the work of [45,46]. These studies build on the earlier work of [47–50] on the use of the digital computer as a tool for optimizing KAM estimates. See also the recent work of [51] on a general approach to computer-assisted

proofs for invariant tori. Note that in the studies just mentioned, the invariant tori are constructed explicitly via Fourier series approximation. Another, more existential approach to KAM theorem is found in the work of [52], where the authors use methods of rigorous numerical integration in order to compute normal forms about periodic orbits of Hamiltonian systems and check the conditions of abstract stability theorems. Using these techniques they show for example that the rotating figure eight choreography orbit in the full three body problem is KAM stable.

We refer also to the work of [53] on the destruction of invariant tori in the planar circular restricted three body problem and the study of [54] on diffusion in a Sun-Jupiter-Asteroid problem.

The study of irregular motions usually focuses on transverse homoclinic/heteroclinic chaos or on the existence of topological horseshoes. See for example the studies of [55–57] on connecting orbits and chaos between periodic orbits in the circular restricted three body problem. See also the work of [58] on transverse intersection between the stable/unstable manifold of such orbits. The recent work of [41] establishes the existence of transverse homoclinic orbits, and hence chaotic motions, for a saddle-focus equilibrium in the CRFBP.

2.4 A-posteriori existence and computer-assisted proof in nonlinear analysis

We now state a theorem which provides sufficient conditions for the existence of a zero to a nonlinear equation, provided one has a good enough, non-degenerate approximate solution. The theorem makes precise the meaning of the terms "good enough" and "non-degenerate", and provides computable conditions for checking these conditions. The reader will find similar theorems with their proofs in the references [26,36,59–62].

Theorem 1 (Radii polynomial approach) *Let X and Y be Banach spaces, $F\colon X \to Y$ be a twice Fréchet differentiable mapping and $\bar{x} \in X$ (typically a numerical approximation). Denote by $\|\cdot\|_X$ the norm on X, $\overline{B_r(\bar{x})} = \{x \in X : \|x - \bar{x}\| \leq r\}$ the closed ball centered at $\bar{x}$, and $\|\cdot\|_{B(X)}$ the bounded linear operator norm. Suppose that $A^\dagger\colon X \to Y$ and $A\colon Y \to X$ are bounded linear operators, and that A is one-to-one (injective). Assume that there are constants $Y_0, Z_0, Z_1 \geq 0$ and a positive function $Z_2\colon (0,\infty) \to (0,\infty)$ having that*

$$\|AF(x)\|_X \leq Y_0, \tag{2}$$

$$\|Id_X - AA^\dagger\|_{B(X)} \leq Z_0, \tag{3}$$

$$\|A\left(DF(\bar{x}) - A^\dagger\right)\|_{B(X)} \leq Z_1, \tag{4}$$

$$\|A\left(DF(x) - DF(\bar{x})\right)\|_{B(X)} \leq Z_2(r)r, \qquad \text{for } x \in \overline{B_r(\bar{x})}. \tag{5}$$

Define the function

$$p(r) \stackrel{\text{def}}{=} Z_2(r)r^2 - (1 - Z_0)r + Y_0. \tag{6}$$

If there exists an $r_0 > 0$ so that $p(r_0) < 0$, then there exists a unique $\tilde{x} \in B_r(\bar{x})$ such that $F(\tilde{x}) = 0$.

Remark 2 In many applications the function $Z_2(r)$ is a polynomial in r. In this case $p(r)$ is a polynomial which we refer to as the radii polynomial. This happens in particular when F is a polynomial map on a product of Banach algebras, the case considered in the present work.

3 Automatic differentiation for the CRFBP: the equivalent polynomial system

In this section we derive a nine dimensional polynomial vector field and show that periodic solutions of the new problem correspond to periodic solutions of the six dimensional CRFBP. The polynomial vector field is obtained by *automatic differentiation*, a process by which we add algebraic differential equations to our system whose solutions correspond to the original non-polynomial nonlinearity.

The idea of replacing a given nonlinear system of differential equation with a polynomial vector field is not new. Examples of using this idea to simplify the development of Taylor integration schemes for celestial mechanics problems appear in the literature as early as the works of [63–65]. In the context of computer-assisted proofs it is important to describe precisely the relationship between the original and the polynomial problems. (The problems are not strictly speaking equivalent, for example in addition to being of different dimensions the polynomial problem is entire and the later has singularities at the locations of the primaries). The study of [41] presents a dynamical systems approach to justifying the automatic differentiation, which we recapitulate below.

3.1 The infinitesimal conjugacy equation

Let $U \subset \mathbb{R}^M$ be an open subset and $f\colon U \to \mathbb{R}^M$ be a smooth non-polynomial vector field. We seek an $N > 0$, a smooth function $h\colon U \subset \mathbb{R}^M \to \mathbb{R}^N$, and a *polynomial* vector field $g\colon \mathbb{R}^{M+N} \to \mathbb{R}^{M+N}$ with

$$\begin{pmatrix} f(\mathbf{x}) \\ Dh(\mathbf{x})f(\mathbf{x}) \end{pmatrix} = g(\mathbf{x}, h(\mathbf{x})), \qquad \mathbf{x} \in U. \tag{7}$$

Defining $R\colon U \to \mathbb{R}^{M+N}$ by

$$R(\mathbf{x}) = \begin{pmatrix} \mathbf{x} \\ h(\mathbf{x}) \end{pmatrix},$$

we see that Equation (7) is equivalent to the infinitesimal conjugacy equation

$$DR(\mathbf{x})f(\mathbf{x}) = g(R(\mathbf{x})), \tag{8}$$

for $\mathbf{x} \in U \subset \mathbb{R}^M$. The dynamical interpretation of Equation (8) is that the vector field g restricted to the graph of h is equivalent to the vector field f pushed forward by R, so that orbits of g on the graph of h correspond to orbits of f. Indeed, the following Lemma is proven in [41].

Lemma 1 *Suppose that f, g, R are as above.*

- *Then the image of R, that is the graph of h, is an invariant manifold for the flow generated by g.*
- *Let $\pi_M\colon \mathbb{R}^{M+N} \to \mathbb{R}^M$ denote projection onto the first M components. Then, if $u\colon [0,T] \to \mathbb{R}^{M+N}$ is a solution of the differential equation $\dot{u} = g(u)$ we have that*

$$\mathbf{x}(t) \stackrel{\text{def}}{=} \pi_M(u(t))$$

is a solution of the differential equation $\dot{\mathbf{x}} = f(\mathbf{x})$ with initial conditions $\pi_M(u(0))$.

In a particular problem involving a non-polynomial vector field f the challenge is to find g and h. The procedure for this is straightforward when f contains N non-polynomial terms which are themselves solutions of polynomial ordinary differential equations. This procedure is best illustrated by considering particular examples. We note that this approach to automatic differentiation of vector fields is a generalization of the approach developed for Taylor series more commonly discussed in the literature (as for example in [66–68]). This approach has the virtue of applying also to basis such as Fourier and Chebyshev as well as for Taylor series. See [27,69] and the discussion below.

3.2 Automatic differentiation for the CRFBP

Returning to the equations of motion for the CRFBP defined in Section 2.1, we define variables

$$u_1 \stackrel{\text{def}}{=} x, \quad u_2 \stackrel{\text{def}}{=} \dot{x}, \quad u_3 \stackrel{\text{def}}{=} y, \quad u_4 \stackrel{\text{def}}{=} \dot{y}, \quad u_5 \stackrel{\text{def}}{=} z, \quad u_6 \stackrel{\text{def}}{=} \dot{z},$$

and

$$u_7 \stackrel{\text{def}}{=} \frac{1}{r_1}, \quad u_8 \stackrel{\text{def}}{=} \frac{1}{r_2}, \quad \text{and} \quad u_9 \stackrel{\text{def}}{=} \frac{1}{r_3},$$

where

$$\begin{aligned} r_1 &= \sqrt{(x-x_1)^2 + (y-y_1)^2 + z^2}, \\ r_2 &= \sqrt{(x-x_2)^2 + (y-y_2)^2 + z^2}, \\ r_3 &= \sqrt{(x-x_3)^2 + (y-y_3)^2 + z^2}. \end{aligned}$$

Recall that (x_j, y_j) for $j = 1, 2, 3$ are the coordinates of the three primary bodies. The virtue of these variables is seen by observing that

$$\begin{aligned} \Omega_x &= x - \frac{m_1(x-x_1)}{r_1^3} - \frac{m_2(x-x_2)}{r_2^3} - \frac{m_3(x-x_3)}{r_3^3} \\ &= u_1 - m_1(u_1 - x_1)u_7^3 - m_2(u_1 - x_2)u_8^3 - m_3(u_1 - x_3)u_9^3, \\ \Omega_y &= y - \frac{m_1(y-y_1)}{r_1^3} - \frac{m_2(y-y_2)}{r_2^3} - \frac{m_3(y-y_3)}{r_3^3} \\ &= u_3 - m_1(u_3 - y_1)u_7^3 - m_2(u_3 - y_2)u_8^3 - m_3(u_3 - y_3)u_9^3, \\ \Omega_z &= -\frac{m_1 z}{r_1^3} - \frac{m_2 z}{r_2^3} - \frac{m_3 z}{r_3^3} \\ &= -m_1 u_5 u_7^3 - m_2 u_5 u_8^3 - m_3 u_5 u_8^3. \end{aligned}$$

That is, the CRFBP nonlinearities are polynomial in the new variables.

To understand the dynamics in terms of these new variables, consider for example that

$$\begin{aligned}\dot{u}_7 &= \frac{-1}{r_1^2}\dot{r}_1 \\ &= \frac{-1}{r_1^2}\frac{d}{dt}\sqrt{(x(t)-x_1)^2+(y(t)-y_1)^2+z(t)^2} \\ &= \frac{-1}{r_1^2}\frac{\frac{d}{dt}(x(t)-x_1)^2+(y(t)-y_1)^2+z(t)^2}{2\sqrt{(x(t)-x_1)^2+(y(t)-y_1)^2+z(t)^2}} \\ &= -(u_1-x_1)u_2u_7^3-(u_3-y_1)u_4u_7^3-u_5u_6u_7^3,\end{aligned}$$

and similarly that

$$\begin{aligned}\dot{u}_8 &= -(u_1-x_2)u_2u_8^3-(u_3-y_2)u_4u_8^3-u_5u_6u_8^3, \\ \dot{u}_9 &= -(u_1-x_3)u_2u_9^3-(u_3-y_3)u_4u_9^3-u_5u_6u_9^3.\end{aligned}$$

Based on these considerations, let $\mathbf{x} \stackrel{\text{def}}{=} (u_1,\ldots,u_6) \in \mathbb{R}^6$ and define the set

$$U = \left\{\mathbf{x}=(u_1,\ldots,u_6) : u_1 \neq x_j \text{ and } u_3 \neq y_j \text{ for } j=1,2,3\right\}.$$

Define the smooth function $h\colon U \subset \mathbb{R}^6 \to \mathbb{R}^3$ by

$$h(\mathbf{x}) = \begin{pmatrix} \frac{1}{\sqrt{(u_1-x_1)^2+(u_3-y_1)^2+u_5^2}} \\ \frac{1}{\sqrt{(u_1-x_2)^2+(u_3-y_2)^2+u_5^2}} \\ \frac{1}{\sqrt{(u_1-x_3)^2+(u_3-y_3)^2+u_5^2}} \end{pmatrix}$$

and let $u = (u_1,\ldots,u_9) \stackrel{\text{def}}{=} R(\mathbf{x}) = (\mathbf{x}, h(\mathbf{x})) \in \mathbb{R}^9$, where $R\colon U \to \mathbb{R}^9$ is smooth. Finally let the polynomial vector field $g\colon \mathbb{R}^9 \to \mathbb{R}^9$ given by

$$g(u) \stackrel{\text{def}}{=} \begin{pmatrix} u_2 \\ 2u_4+u_1-m_1(u_1-x_1)u_7^3-m_2(u_1-x_2)u_8^3-m_3(u_1-x_3)u_9^3 \\ u_4 \\ -2u_2+u_3-m_1(u_3-y_1)u_7^3-m_2(u_3-y_2)u_8^3-m_3(u_3-y_3)u_9^3 \\ u_6 \\ -m_1u_5u_7^3-m_2u_5u_8^3-m_3u_5u_9^3 \\ -(u_1-x_1)u_2u_7^3-(u_3-y_1)u_4u_7^3-u_5u_6u_7^3 \\ -(u_1-x_2)u_2u_8^3-(u_3-y_2)u_4u_8^3-u_5u_6u_8^3 \\ -(u_1-x_3)u_2u_9^3-(u_3-y_3)u_4u_9^3-u_5u_6u_9^3 \end{pmatrix}. \quad (9)$$

With g and R so defined it is a straightforward calculation to verify that Equation (8) is satisfied for the CRFBP field f. Recalling Lemma 1 we have the following.

Lemma 2 *If $u = (u_1,\ldots,u_9)\colon [0,T] \to \mathbb{R}^9$ is a T-periodic solution of $\dot{u} = g(u)$, then $\mathbf{x}(t) \stackrel{\text{def}}{=} \pi_6(u(t)) = (u_1,\ldots,u_6)\colon [0,T] \to \mathbb{R}^6$ is a T-periodic solution of the CRFBP $\dot{\mathbf{x}} = f(\mathbf{x})$ with f given in* (1).

3.3 Unfolding parameters

Periodic solutions of the polynomial system defined in Lemma 2 occur in five parameter families, and are hence not isolated. The five unit Floquet multipliers come from

(a) the shift invariance always present when we study periodic solutions of vector fields;
(b) the fact that g inherits a first integral from f;
(c) the fact that each of the three appended equations introduces a spurious periodic family. We say that the extra families are spurious as they lie off the image of R, and hence have nothing to do with the dynamics of the CRFBP. Nevertheless they are present when we study g and have to be understood/excluded.

The degeneracy introduced by (a) is handled by introducing a phase condition. We take a standard Poincaré section. The degeneracy introduced by (b) is handled by fixing the desired frequency/period. This choice must be balanced by introducing an *unfolding parameter* to re-balance the system of equation. This classical technique is discussed for example in the works of [33, 70, 71]. Each degeneracy from (c) is due to the fact that we have to impose that the periodic orbit is on the manifold parameterized by R. We achieve this by introducing three additional scalar constraint equations. Each of these constraint equations must be balanced by its own unfolding parameter, resulting in a total of four. In the end these parameters will end up being zero, as we show below. Their ultimate purpose is to remove the four dimensional kernel – resulting from the degeneracies just mentioned – from the linearized problem.

More precisely then, we let $\alpha_1, \alpha_2, \alpha_3, \beta \in \mathbb{R}$ the *unfolding parameters* and consider the augmented system of equations

$$\begin{aligned}
\dot{u}_1 &= u_2 \\
\dot{u}_2 &= 2u_4 + u_1 - m_1(u_1 - x_1)u_7^3 - m_2(u_1 - x_2)u_8^3 - m_3(u_1 - x_3)u_9^3 + \beta u_2 \\
\dot{u}_3 &= u_4 \\
\dot{u}_4 &= -2u_2 + u_3 - m_1(u_3 - y_1)u_7^3 - m_2(u_3 - y_2)u_8^3 - m_3(u_3 - y_3)u_9^3 \\
\dot{u}_5 &= u_6 \\
\dot{u}_6 &= -m_1u_5u_7^3 - m_2u_5u_8^3 - m_3u_5u_9^3 \\
\dot{u}_7 &= -(u_1 - x_1)u_2u_7^3 - (u_3 - y_1)u_4u_7^3 - u_5u_6u_7^3 + \alpha_1u_7^3 \\
\dot{u}_8 &= -(u_1 - x_2)u_2u_8^3 - (u_3 - y_2)u_4u_8^3 - u_5u_6u_8^3 + \alpha_2u_8^3 \\
\dot{u}_9 &= -(u_1 - x_3)u_2u_9^3 - (u_3 - y_3)u_4u_9^3 - u_5u_6u_9^3 + \alpha_3u_9^3
\end{aligned} \tag{10}$$

Denote $\alpha = (\alpha_1, \alpha_2, \alpha_3) \in \mathbb{R}^3$, and denoting the right hand side of (10) by $\tilde{g}(u, \beta, \alpha)$, we get

$$\tilde{g}(u, \beta, \alpha) \overset{\text{def}}{=} g(u) + \begin{pmatrix} 0 \\ \beta u_2 \\ 0 \\ 0 \\ 0 \\ 0 \\ \alpha_1 u_7^3 \\ \alpha_2 u_8^3 \\ \alpha_3 u_9^3 \end{pmatrix}.$$

We have the following lemma, which is related to the results of [33]. Since the lemma does not exactly follow directly from any of the classical results, we include the proof – which involves some tedious calculations – in the Appendix A for the sake of completeness.

Lemma 3 *Assume that $\alpha_1, \alpha_2, \alpha_3, \beta, \omega \in \mathbb{R}$ are fixed constants with $\omega > 0$, and let $\mathbf{n}, \mathbf{p} \in \mathbb{R}^9$ be fixed vectors. Let $T = 2\pi/\omega$. Suppose that $u = (u_1, \ldots, u_9)\colon [0, T] \to \mathbb{R}^9$ is a T-periodic solution of $\dot{u} = \tilde{g}(u, \beta, \alpha)$ with*

$$\begin{aligned} 0 &= (u(0) - \mathbf{p}) \cdot \mathbf{n} \\ u_7(0) &= \frac{1}{\sqrt{(u_1(0) - x_1)^2 + (u_3(0) - y_1)^2 + u_5(0)^2}} \\ u_8(0) &= \frac{1}{\sqrt{(u_1(0) - x_2)^2 + (u_3(0) - y_2)^2 + u_5(0)^2}} \\ u_9(0) &= \frac{1}{\sqrt{(u_1(0) - x_3)^2 + (u_3(0) - y_3)^2 + u_5(0)^2}} \end{aligned} \tag{11}$$

and that $u_7(t), u_8(t), u_9(t) > 0$ for all $t \in [0, T]$. Then

(i) $\alpha_1 = \alpha_2 = \alpha_3 = \beta = 0$, and
(ii) the function $\mathbf{x} \stackrel{\text{def}}{=} (u_1, \ldots, u_6)\colon [0, T] \to \mathbb{R}^6$ is a T-periodic solution of the circular restricted four body problem $\dot{\mathbf{x}} = f(\mathbf{x})$ with f given in (1).

4 The rigorous computational approach based on Chebyshev series

Based on the analysis provided by the previous section, we now define a nonlinear Chebyshev operator equation of the form $F(x) = 0$ on a Banach space of infinite sequences whose zeros correspond to periodic orbits of $\dot{u} = \tilde{g}(u, \beta, \alpha)$, and via Lemma 3 to periodic orbits of the CRFBP. To define the Chebyshev operator, we employ the techniques described in the paper [28], following closely their notation and approach. Once the operator is obtained, we will apply the *radii polynomial approach* (as described in Theorem 1) to prove existence of solutions of $F(x) = 0$.

As in [28], considering any partition of $[0, 1]$

$$\mathcal{P}_m \stackrel{\text{def}}{=} \{t_0 = 0 < t_1 < t_2 < \cdots < t_{m-1} < t_m = 1\}, \tag{12}$$

where $m \in \mathbb{N}$ is the mesh size. Fix $\omega > 0$, and let $\mathbf{n}, \mathbf{p} \in \mathbb{R}^9$ be fixed vectors. Looking for periodic orbits of (10) is equivalent to

$$(\mathbf{P}_1)\begin{cases} \dfrac{d}{dt}u^{(1)}(t) = \dfrac{1}{\omega}\tilde{g}(u^{(1)}(t), \beta, \alpha), \quad t \in [0, t_1], \\ u^{(1)}(0) = u^{(m)}(1), \\ (u^{(1)}(0) - \mathbf{p}) \cdot \mathbf{n} = 0, \\ (u_7^{(1)}(0))^2 \left((u_1^{(1)}(0) - x_1)^2 + (u_3^{(1)}(0) - y_1)^2 + (u_5^{(1)}(0))^2 \right) = 1, \\ (u_8^{(1)}(0))^2 \left((u_1^{(1)}(0) - x_2)^2 + (u_3^{(1)}(0) - y_2)^2 + (u_5^{(1)}(0))^2 \right) = 1, \\ (u_9^{(1)}(0))^2 \left((u_1^{(1)}(0) - x_3)^2 + (u_3^{(1)}(0) - y_3)^2 + (u_5^{(1)}(0))^2 \right) = 1. \end{cases}$$

$$(\mathbf{P}_i)\begin{cases} \dfrac{d}{dt}u^{(i)}(t) = \dfrac{1}{\omega}\tilde{g}(u^{(i)}(t), \beta, \alpha), \quad t \in [t_{i-1}, t_i], \\ u^{(i)}(t_{i-1}) = u^{(i-1)}(t_{i-1}), \end{cases} \quad \text{for } i = 2, \ldots, m,$$

where $u^{(i)} : [t_{i-1}, t_i] \to \mathbb{R}^n$ is a solution of the differential equation $\dot{u} = \frac{1}{\omega}\tilde{g}(u, \beta, \alpha)$ on the time interval $[t_{i-1}, t_i]$ for $i = 1, 2, \ldots, m$. The idea of the approach is to solve each problem $(\mathbf{P}_i)$ on the time interval $[t_{i-1}, t_i]$ for each $i = 1, 2, \ldots, m$ using Chebyshev series expansions of each component $u_k^{(i)}$ $(k = 1, \ldots, 9)$ of the solutions. As we shall see, solving simultaneously all problems $(\mathbf{P}_1)$, …, $(\mathbf{P}_m)$ using Chebyshev series will lead to the equivalent zero finding problem $F(x) = 0$ posed on a Banach space of infinite sequences of Chebyshev coefficients.

For each time subdomain index $i = 1, \ldots, m$, let $\sigma_i : [-1, 1] \to [t_{i-1}, t_i]$ be given by

$$\sigma_i(t) \overset{\text{def}}{=} \frac{t_i - t_{i-1}}{2}(t + 1) + t_{i-1}, \tag{13}$$

and let $\tilde{u}^{(i)} : [-1, 1] \to \mathbb{R}^9$ be given by $\tilde{u}^{(i)}(t) \overset{\text{def}}{=} u^{(i)}(\sigma_i(t))$. Hence, if $u^{(i)}$ is a solution of the differential equation $\dot{u} = \frac{1}{\omega}\tilde{g}(u, \beta, \alpha)$ on the time interval $[t_{i-1}, t_i]$, then $\tilde{u}^{(i)}$ is a solution of the differential equation $\dot{u} = \frac{t_i - t_{i-1}}{2\omega}\tilde{g}(u, \beta, \alpha)$ on the time interval $[-1, 1]$. Given any $i \in \{1, \ldots, m\}$ and $j \in \{1, \ldots, 9\}$, expand $\tilde{u}_j^{(i)} : [-1, 1] \to \mathbb{R}$ in Chebyshev series as

$$\tilde{u}_j^{(i)}(t) = [a_j^{(i)}]_0 + 2\sum_{k=1}^{\infty} [a_j^{(i)}]_k T_k(t), \qquad t \in [-1, 1], \tag{14}$$

and denote $a_j^{(i)} = \left([a_j^{(i)}]_k \right)_{k \geq 0}$ the infinite sequence of Chebyshev coefficients of $\tilde{u}_j^{(i)}$. Moreover, given $i \in \{1, \ldots, m\}$ denote $a^{(i)} = \left(a_1^{(i)}, a_2^{(i)}, \ldots, a_9^{(i)} \right)$, the vector containing the infinite sequences of Chebyshev coefficients of each of the nine components of the solution $\tilde{u}^{(i)} : [-1, 1] \to \mathbb{R}^9$.

Given a number $\rho \geq 0$ and a sequence of real numbers $c = (c_k)_{k \geq 0}$ define the weighed ℓ^1 norm

$$\|c\|_{(\rho,1)} \overset{\text{def}}{=} |c_0| + 2\sum_{k=1}^{\infty} |c_k| \rho^k.$$

Given $n \in \mathbb{N}$, define the sequence space

$$\ell^1_{(\rho,n)} \overset{\text{def}}{=} \left\{ a = (a_1, a_2, \ldots, a_n) \;\middle|\; a_j = \left([a_j]_k \right)_{k \geq 0} \text{ and } \|a_j\|_{(\rho,1)} < \infty,\ 1 \leq j \leq n \right\}.$$

The sequence space $\ell^1_{(\rho,n)}$ is endowed with the norm

$$\|a\|_{(\rho,n)} \stackrel{\text{def}}{=} \max_{j=1,\dots,n} \left\{ \|a_j\|_{(\rho,1)} = |[a_j]_0| + 2\sum_{k=1}^{\infty} |[a_j]_k| \rho^k \right\}.$$

Given a sequence of *decay rates* $\nu = (\nu_i)_{i=1}^m \in \mathbb{R}_+^m$, denote the Banach space

$$X_\nu \stackrel{\text{def}}{=} \mathbb{R}^4 \times \prod_{i=1}^m \ell^1_{(\nu_i,n)}.$$

The norm $\|\cdot\|_{X_\nu}$ on the space X_ν is defined as follows. Given

$$x = (\beta, \alpha, a^{(1)}, \dots, a^{(m)}) \in \mathbb{R}^4 \times \prod_{i=1}^m \ell^1_{(\nu_i,n)} = X_\nu,$$

its norm is given by

$$\|x\|_{X_\nu} = \max \left\{ |\beta|, |\alpha_1|, |\alpha_2|, |\alpha_3|, \|a^{(1)}\|_{(\nu_1,n)}, \|a^{(2)}\|_{(\nu_2,n)}, \dots, \|a^{(m)}\|_{(\nu_m,n)} \right\}.$$

Definition 1 (Chebyshev operator for periodic orbits) Let $\nu = (\nu_i)_{i=1}^m$ and $\tilde{\nu} = (\tilde{\nu}_i)_{i=1}^m$ be some weights with $1 < \tilde{\nu}_i < \nu_i$ for all $i = 1, \dots, m$. Fix $\omega > 0$ and two vectors $\mathbf{n}, \mathbf{p} \in \mathbb{R}^9$. The *Chebyshev operator for periodic orbits* is the mapping $F : X_\nu \to X_{\tilde{\nu}}$ defined by

$$F(x) = \left(F_0(a^{(1)}), F_1(\beta, \alpha, a^{(m)}, a^{(1)}), F_2(\beta, \alpha, a^{(1)}, a^{(2)}), \dots, F_m(\beta, \alpha, a^{(m-1)}, a^{(m)}) \right),$$

where $F_0 : \ell^1_{(\nu_1,n)} \to \mathbb{R}^4$, and $F_i : \mathbb{R}^4 \times \ell^1_{(\nu_{i-1},n)} \times \ell^1_{(\nu_i,n)} \to \ell^1_{(\tilde{\nu}_i,n)}$ are given by

$$F_0(a^{(1)}) \stackrel{\text{def}}{=} \begin{cases} \sum_{j=1}^{9} \left([a_j^{(1)}]_0 + 2\sum_{k=1}^{N-1} (-1)^k [a_j^{(1)}]_k - \mathbf{p}_j \right) \mathbf{n}_j \\ (u_7^{(1)}(0))^2 \left((u_1^{(1)}(0) - x_1)^2 + (u_3^{(1)}(0) - y_1)^2 + (u_5^{(1)}(0))^2 \right) - 1 \\ (u_8^{(1)}(0))^2 \left((u_1^{(1)}(0) - x_2)^2 + (u_3^{(1)}(0) - y_2)^2 + (u_5^{(1)}(0))^2 \right) - 1 \\ (u_9^{(1)}(0))^2 \left((u_1^{(1)}(0) - x_3)^2 + (u_3^{(1)}(0) - y_3)^2 + (u_5^{(1)}(0))^2 \right) - 1 \end{cases}$$

where for $j = 1, 3, 5, 7, 8, 9$, the $u_j^{(1)}(0) \stackrel{\text{def}}{=} [a_j^{(1)}]_0 + 2\sum_{k\geq 1}(-1)^k [a_j^{(1)}]_k$, and where for $i = 1, \dots, m$

$$F_i(\beta, \alpha, a^{(i-1)}, a^{(i)}) \stackrel{\text{def}}{=} \begin{cases} [a^{(i)}]_0 - [a^{(i-1)}]_0 + 2\sum_{k=1}^{\infty} \left((-1)^k [a^{(i)}]_k - [a^{(i-1)}]_k \right), & k = 0 \\ \omega k [a^{(i)}]_k - \frac{t_i - t_{i-1}}{4} \left([\phi^{(i)}]_{k-1} - [\phi^{(i)}]_{k+1} \right), & k \geq 1, \end{cases}$$

where we set $a^{(0)} = a^{(m)}$, and where $\phi^{(i)} = \phi^{(i)}(\beta, \alpha, a^{(i)})$ represents the Chebyshev coefficients of $\tilde{g}(u^{(i)}, \beta, \alpha)$, that is for $j = 1, \dots, 9$

$$\tilde{g}_j(u^{(i)}(t), \beta, \alpha) = [\phi_j^{(i)}]_0 + 2\sum_{k=1}^{\infty} [\phi_j^{(i)}]_k T_k(t), \qquad t \in [-1, 1].$$

Lemma 4 *Fix $\omega > 0$, $\mathbf{p}, \mathbf{n} \in \mathbb{R}^9$, $m \in \mathbb{N}$ and a partition $\mathcal{P}_m$ of $[0,1]$ as in (12). Let $T \stackrel{\text{def}}{=} 1/\omega$. Consider the Chebyshev operator as defined in Definition 1. Let $\nu = (\nu_i)_{i=1}^m$ and assume that $x = (\beta, \alpha, a^{(1)}, \dots, a^{(m)}) \in X_\nu$ satisfies $F(x) = 0$. For each $i = 1, \dots, m$, define $\tilde{u}^{(i)} : [-1,1] \to \mathbb{R}^9$ component-wise by (14). Recall (13) and define $u : [0,T] \to \mathbb{R}^9$ component-wise (that is for $j = 1, \dots, 9$) by*

$$u_j(t) \stackrel{\text{def}}{=} \tilde{u}_j^{(i)}(\sigma_i(t/T)), \quad \text{if } t/T \in [t_{i-1}, t_i] \subset [0,1].$$

Then $u : [0,T] \to \mathbb{R}^9$ is a T-periodic solution of $\dot{u} = \tilde{g}(u, \beta, \alpha)$ satisfying the four conditions (11). Moreover, $\mathbf{x}(t) \stackrel{\text{def}}{=} \pi_6(u(t)) = (u_1, \dots, u_6) : [0,T] \to \mathbb{R}^6$ is a T-periodic solution of the CRFBP $\dot{\mathbf{x}} = f(\mathbf{x})$ with f given in (1).

Based on the analysis of Lemma 4, a vector $x \in X_\nu$ satisfying $F(x) = 0$ defines a periodic orbit in the CRFBP. Finally, obtaining computer-assisted proofs of existence of periodic orbits in the CRFBP boils down to applying the radii polynomial approach (as presented in Theorem 1) to compute rigorously solutions of $F = 0$. To apply Theorem 1, we need the following ingredients: a numerical approximation $\bar{x}$, an approximate derivative $A^\dagger$ of $DF(\bar{x})$, an approximate inverse A of $DF(\bar{x})$ and the bounds Y_0, Z_0, Z_1 and Z_2 satisfying respectively (2), (3), (4) and (5). The construction of these ingredients is standard in the field of rigorous numerics in dynamics, and we refer to the paper [28] for their explicit derivation. Perhaps the only difference with the approach of [28] is the way we compute the discrete convolutions involved in the components of the Chebyshev operator F. The next remark provides details about this.

Remark 3 (Controlling the numerical instability of weighted ℓ^1 norms) To define Y_0 satisfying (2), we must compute rigorously an upper bound for $\|AF(\bar{x})\|_{X_\nu}$. This computation involves controlling weighted ℓ^1 norms of the terms $\phi^{(i)} = \left([\phi^{(i)}]_k\right)_{k \geq 0}$ in the definition of F_i. Since the terms in $\phi^{(i)}$ are defined by cubic, quartic and quintic convolutions, the computation of their weighted ℓ^1 norms can be unstable numerically, especially when the vector of decay rates $\nu \in \mathbb{R}_+^m$ has large components (which is often necessary to show that the bound Z_1 satisfying in (4) is such that $Z_1 < 1$ - a necessary condition for the radii polynomial approach to succeed). To control this numerical instability, we used the method introduced in [29] (which combines the FFT algorithm and the property that the sequence space $\ell^1_{(\rho,1)}$ is a Banach algebra under discrete convolutions) to compute rigorous enclosure of discrete convolutions which decay exponentially fast. This approach stabilizes the computation of the norms in $\ell^1_{(\rho,1)}$ of the components of the Chebyshev operator F.

We are now ready to present several computer-assisted proofs of existence of periodic orbits in the CRFBP.

5 Results

Using the interval arithmetic MATLAB package INTLAB [72], we wrote a computer program implementing a rigorous implementation of the bounds Y_0, Z_0, Z_1 and Z_2 satisfying (2), (3), (4) and (5), respectively. For a selection of numerical approximations $\bar{x}$ obtained using our continuation scheme, we proved the existence of $r > 0$ such that the radii polynomial p defined in (6) satisfy $p(r) < 0$. The number r is the radius of the

closed ball about $\bar{x}$ $\overline{B_r(\bar{x})} \subset X_\nu$ which contains a unique solution $\tilde{x}$ of the Chebyshev operator equation $F(x) = 0$. Moreover, the radius r provides a C^0 error between the numerical approximation $\bar{u} : [0, T] \to \mathbb{R}^9$ and the true periodic solution $\tilde{u} : [0, T] \to \mathbb{R}^9$.

5.1 Vertical Lyapunov families for equal masses

Beginning with the known equilibrium solutions given by the libration points, the vertical Lyapunov families provide a natural starting point in the study of spatial periodic orbits. Indeed each libration points in the CRFBP has a pair of purely imaginary eigenvalues associated with the out of plane eigenvectors, and we expect these imaginary eigenvalues to give rise to a one parameter family of periodic out of plane oscillations referred to as a vertical Lyapunov family. This family can be computed very accurately near the libration point using a center manifold reduction as discussed in [31]. Beginning from an orbit in the center manifold we apply a standard numerical continuation scheme and follow the branch. This leads to a large number of numerical orbits, some of which we take as input to our computer assisted proof.

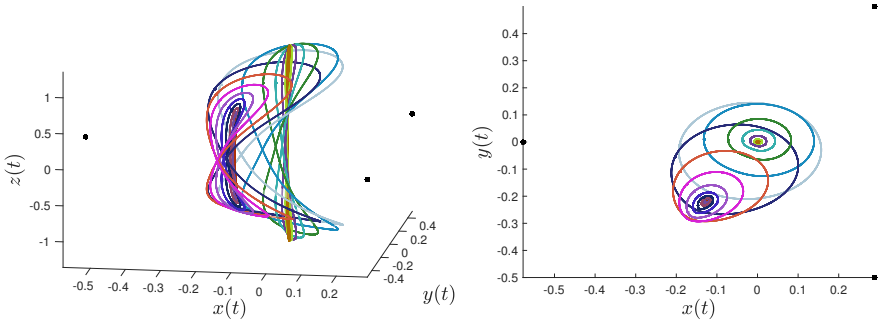

Fig. 5 (**left**) L_1 family of periodic orbits. (**right**) The projection of the same family in the $x-y$ plane. The family appears to accumulate on the z-axis, probably joining with the vertical family associated with L_0.

Figure 5 and Table 1 illustrate the results obtained by applying this strategy at the libration point L_1 in the triple Copenhagen problem ($m_1 = m_2 = m_3 = 1/3$). For each orbit we record an approximate initial condition, the approximate period, and the computer assisted C^0 error bound resulting from our a-posteriori analysis. We note that the vertical family at L_1 appears to accumulate at the vertical family at L_0 – the libration point at the origin. The L_0 family lies entirely on the z-axis, as the axis is invariant in the triple Copenhagen problem (that is, there is a four body version of the Sitnikov problem at the origin). Due to the rotational symmetry of the triple Copenhagen problem, the vertical families at the remaining inner libration points L_2 and L_3 are obtained by a rotation of $\pm 2\pi/3$ radians.

Analogous results are given for the vertical Lyapunov families associated with the outer libration points L_4 and L_7 of the triple Copenhagen problem in Figure 6/Table 2, and Figure 7/Table 3 respectively. These families appear to pass through the plane of the primaries. We remark that related spatial families of periodic orbits for the CRFBP

x_0	y_0	z_0	T	r
−0.122289225462523	−0.207533311065121	0.529138349856541	4.054855053094634	1.0187×10^{-12}
−0.125085701176184	−0.208191879625059	0.562688265866234	4.276831795726809	2.1287×10^{-12}
−0.129235586222753	−0.207861153248102	0.594973385794514	4.524519594269676	4.2954×10^{-12}
−0.135374107266786	−0.205326538415879	0.626051803502019	4.802660136913967	1.1914×10^{-11}
−0.144389309793357	−0.198454441674160	0.656267080975480	5.117237446282061	2.0433×10^{-11}
−0.157291376568209	−0.183669361400241	0.686221795529157	5.475913266026079	1.2455×10^{-10}
−0.174343299267986	−0.155806168723353	0.716315828539586	5.888659350596167	5.2109×10^{-11}
−0.192595093185209	−0.111202948542675	0.745453620813919	6.368699018104573	1.642×10^{-10}
−0.203642493817956	−0.056501618546415	0.770903270735781	6.933950105858384	2.0111×10^{-10}
−0.191811339407319	−0.009696632351101	0.792290338287996	7.609311182033357	6.5094×10^{-10}
−0.132364862071404	0.008870843741732	0.810343110978991	8.301357570042617	9.3382×10^{-10}
−0.072666504343116	0.007051710472639	0.818842318120466	8.636744551142441	3.1719×10^{-9}
−0.037132590842156	0.003949576292829	0.822191519222494	8.777476738910274	1.1234×10^{-9}
−0.018346086869568	0.002019445948951	0.823554651873667	8.840385931394222	1.8856×10^{-9}
−0.008013858390257	0.000896423611318	0.824190092968421	8.872179901905529	1.1786×10^{-9}
−0.003086310278375	0.000347689187209	0.824465021943802	8.886701395424178	9.9955×10^{-10}

Table 1 Data for the proofs of the L_1 periodic orbits: the table reports an approximate initial condition, an approximate period, and a bound on the C^0 distance from the approximate to the true solution. This bound is certified via computer assisted proof.

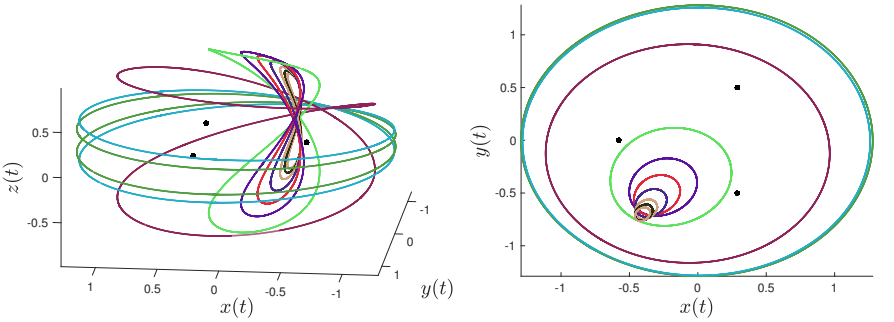

Fig. 6 (**left**) L_4 family of periodic orbits. The periods of the periodic orbits vary from 5.5916 to 7.2211. (**right**) The projection of the same family in the $x - y$ plane.

x_0	y_0	z_0	T	r
−0.383763890245742	−0.637680682274115	0.523470497931155	5.591549225334269	4.9619×10^{-13}
−0.370356974592502	−0.609388576507564	0.560612351451114	5.616324781838816	3.4915×10^{-13}
−0.348524700969929	−0.562437235782292	0.615089199486379	5.661447598130970	4.4863×10^{-13}
−0.304681919062111	−0.463582639243643	0.708996594994930	5.774345851340401	4.7384×10^{-13}
−0.251816056211873	−0.330637443216791	0.806057426307151	5.966480247296522	1.4406×10^{-12}
−0.200717162087890	−0.172080971253182	0.891437747179197	6.237763952263020	2.6675×10^{-12}
−0.137938593006089	0.117236811740925	0.969359551888878	6.658699195155489	1.2652×10^{-11}
−0.027380354672314	0.910056458833169	0.729783958405979	7.106355151280942	1.5106×10^{-10}
0.027646012461087	1.258195860424453	0.238367974966189	7.215123175743175	2.2038×10^{-10}
0.031549363922057	1.280655495512409	0.140489380564831	7.221148008798753	2.6919×10^{-10}

Table 2 Data for the proofs of the L_4 periodic orbits.

were studied numerically in [25]. We also remark that the vertical Lyapunov families at L_5, L_6, L_8 and L_9 are obtained by rotation, giving rise to the data illustrated in Figure 1.

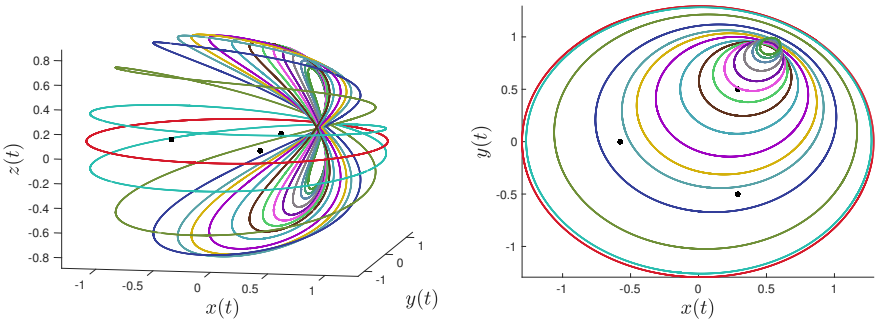

Fig. 7 (**left**) L_7 family of periodic orbits. The periods of the periodic orbits vary from 6.5069 to 7.2274. (**right**) The projection of the same family in the $x-y$ plane.

x_0	y_0	z_0	T	r
0.502689811743375	0.833558905046233	0.486712179371164	4.849388631553417	4.3944×10^{-13}
0.487668791063386	0.800658887491201	0.520099116195402	4.858985107159089	5.0146×10^{-13}
0.469324894579415	0.759914079318071	0.555883606329537	4.872961763719262	6.1456×10^{-13}
0.433694470359655	0.678635720970620	0.613124135736361	4.908955202279222	8.5757×10^{-13}
0.392448700017175	0.580096738324562	0.663947817484059	4.970704528481551	2.6864×10^{-12}
0.356016601551482	0.487852134706820	0.698479110206251	5.051729535003786	4.4742×10^{-12}
0.316576793863261	0.380815951878208	0.728178130298897	5.181291411465808	8.8868×10^{-12}
0.272448541610778	0.250436615121029	0.757200197795193	5.398105522420959	1.5702×10^{-11}
0.219274627884591	0.080531217183134	0.795600211410380	5.757735873281634	4.8019×10^{-11}
0.153278505582348	−0.137679411934353	0.845527639629543	6.219764595936430	1.3925×10^{-10}
0.103253090460576	−0.307206421700990	0.868746879490270	6.506946563175474	2.0281×10^{-10}
0.066361012705998	−0.436649893801542	0.870474420881650	6.680833879377727	2.4829×10^{-10}
0.004361783174264	−0.665967056748814	0.831186386989828	6.911713942743985	2.5986×10^{-10}
−0.082303234694366	−1.015815643672100	0.626980520177040	7.129705249437175	1.623×10^{-10}
−0.135851103131295	−1.250185893007391	0.237019926486067	7.215111487131836	2.7487×10^{-10}
−0.143210577208458	−1.283856816187275	−0.000000000000000	7.227420738171950	1.2821×10^{-10}

Table 3 Data for the proofs of the L_7 periodic orbits.

5.2 A vertical family with non-equal masses

We stress that our method does not make use of any symmetries which may or may not be present in the problem, and because of this it can be used to prove the existence of non-symmetric orbits. To illustrate this we consider the CRFBP with mass values $m_1 = 0.4$, $m_2 = 0.35$, and $m_3 = 0.25$, breaking the symmetry of the triple Copenhagen problem. In this case the z-axis is no longer invariant and we consider the vertical Lyapunov family associated with L_0 (which no longer sits at the origin). After computing the center manifold reduction we perform a numerical continuation of the branch. We prove the existence of 15 periodic orbits obtained in this way. The results are recorded in Figure 8/Table 4.

5.3 Spatial orbits bifurcating from planar Lyapunov families: Halo and Axial Families

We recall that the plane of the primaries is an invariant subspace for the CRFBP. Then another mechanism producing spatial periodic orbits is a symmetry breaking bifurcation for a planar family of periodic orbits [34]. Natural examples include the planar Lyapunov families associated with the libration points. Indeed, studying bifur-

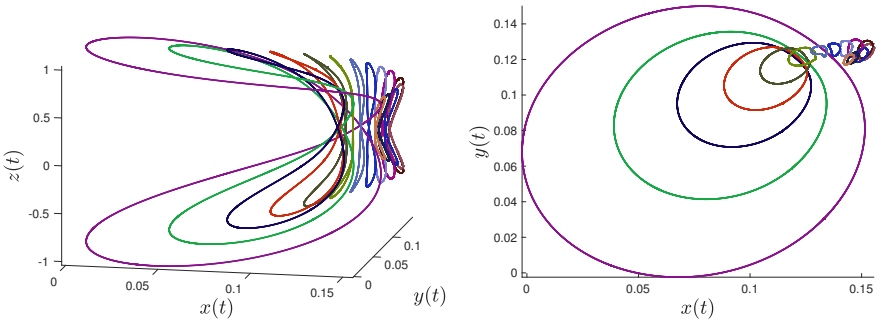

Fig. 8 (**left**) L_0 family of periodic orbits at non equal masses. The periods of the periodic orbits vary from x to y. (**right**) The projection of the same family in the $x-y$ plane.

x_0	y_0	z_0	T	r
0.145491329790451	0.122854791964656	0.322810036658151	3.259541152055203	9.5416×10^{-12}
0.147471200684045	0.123974136543916	0.342881439080876	3.322031071535297	2.0177×10^{-13}
0.151060878184127	0.126345377031743	0.386205252042305	3.470328367789882	2.5533×10^{-13}
0.152965863347815	0.128624867569802	0.432104012963414	3.649021710149416	3.6365×10^{-13}
0.151779087240134	0.130400269119949	0.479992561738977	3.862689096138990	6.0491×10^{-13}
0.146006820921688	0.130842941809327	0.534323307971210	4.147517057122860	1.2486×10^{-12}
0.141024015095218	0.129799078736497	0.564262251795274	4.329965102371600	8.1966×10^{-12}
0.135259386496352	0.127382988398780	0.593192896275441	4.529203417406517	3.352×10^{-12}
0.129136900634573	0.123183269784283	0.620958495755745	4.747661549302546	5.9831×10^{-12}
0.123158853952597	0.116748815297872	0.647439226185944	4.988261539383478	1.0487×10^{-11}
0.117960972883468	0.107609941398706	0.672563105198326	5.254549377063696	1.6948×10^{-11}
0.114414931910950	0.095287245784743	0.696303549275730	5.550870932411943	4.5855×10^{-11}
0.113837282314410	0.079231313442026	0.718673052465518	5.882610974897646	1.1163×10^{-10}
0.118490214884424	0.058510359277878	0.739720249652228	6.256523347646549	2.5314×10^{-10}
0.133094346402133	0.030456620478405	0.759467102372963	6.681195608562205	1.5141×10^{-9}

Table 4 Data for the proofs of the L_0 periodic orbits.

cations from the planar Lyapunov families is known to give rise to spatial halo and axial families in the CRTBP. See for example [73, 74], and the references discussed therein.

Taking the CRFBP with non-equal masses $m_1 = 0.4$, $m_2 = 0.3$ and $m_3 = 0.2$ – the asymmetric example parameters from [15] – we start from L_1 and perform a center manifold reduction for the in plane eigenspace associated with the purely imaginary pair of eigenvalues. As in the previous examples we numerically continue the resulting family until we encounter an out of plane stability bifurcation. That is, we track the Floquet multipliers of the periodic orbit and watch for the first bifurcation associated with the out of plane bundle (Floquet multipliers pass through a root of unity). When this occurs an out of plane family of periodic orbits may be born (in a pitch fork bifurcation) and if so we follow the new family via numerical continuation. This leads for example to the halo family illustrated in Figure 9. The results of a number of computer assisted proofs for this family are given in Table 5.

Following the planar Lyapunov family associated with L_1 past the first bifurcation we find other out of plane bifurcations, giving rise to additional spatial families which can be followed using numerical continuation. Two more such families are illustrated in Figures 10 and 11. Applying our method of proof along these branches leads to the certified data reported in Tables 6 and 7. We have also performed some numerical continuations involving the mass parameters, but we believe that including more results in the present work puts us past the point of diminishing returns. Systematic and

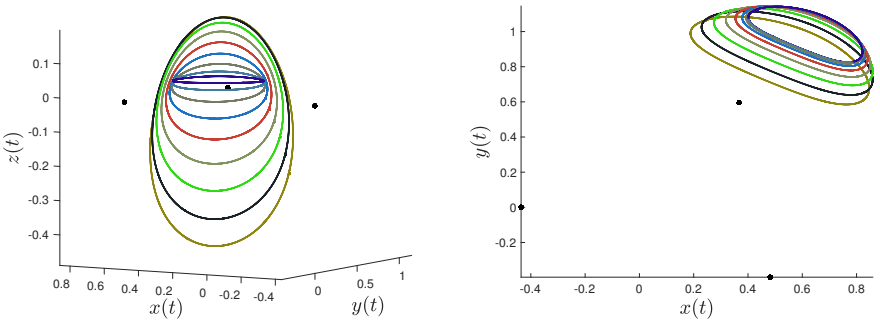

Fig. 9 (**left**) Halo family at the mass ratio $m_1 = 0.5$, $m_2 = 0.3$ and $m_3 = 0.2$. The periods of the periodic orbits vary from 4.40766 to 4.04788. (**right**) The projection of the same family in the $x - y$ plane.

x_0	y_0	z_0	T	r
0.433336478930126	1.126469727457606	−0.008698078879862	4.407664602008706	2.6866×10^{-12}
0.431551505590302	1.126606576660561	−0.018764783368137	4.406326751488494	1.6134×10^{-12}
0.426008536800889	1.126972494920192	−0.035108596007713	4.402067365812841	1.7652×10^{-12}
0.413002593477175	1.127470466449532	−0.058644215867131	4.391421338236864	2.0564×10^{-12}
0.390401969603942	1.127071044068332	−0.088383350585881	4.370505219222184	2.8904×10^{-12}
0.358362738862961	1.123494705949155	−0.124298177639717	4.334428699369387	3.0981×10^{-12}
0.319151461937504	1.113479866053269	−0.166907930691462	4.275868296906199	9.5075×10^{-12}
0.277790352123064	1.093912430511562	−0.215484192050279	4.184773679094075	3.2392×10^{-11}
0.241248984967261	1.063339364664482	−0.267765006277291	4.047880214712584	7.7352×10^{-10}

Table 5 Data for the proofs of the halo periodic orbits.

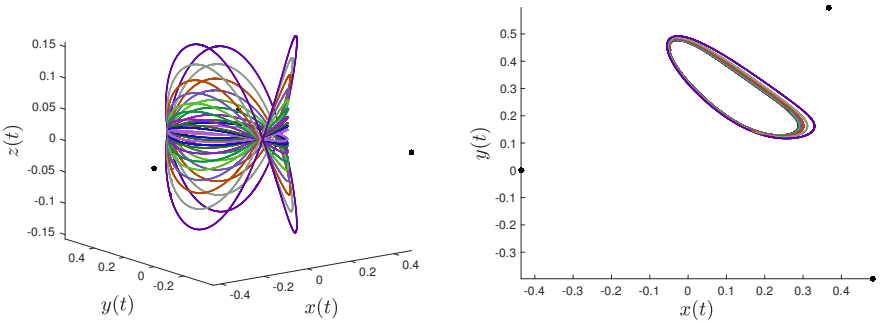

Fig. 10 (**left**) Axial family at the mass ratio $m_1 = 0.5$, $m_2 = 0.3$ and $m_3 = 0.2$. The periods of the periodic orbits vary from 7.9168 to 8.2118. (**right**) One axial periodic solution with frequency $\omega \approx 0.121776$, that is with period about 8.2118.

mathematically rigorous study of continuous branches of periodic orbits – and their bifurcations – in the CRFBP varying mass and energy parameters would make an interesting topic of future study. Just such a study for the Halo Orbits in the restricted three body has been conducted by [44], and it seems that those methods could be applied to the CRFBP as well.

x_0	y_0	z_0	T	r
−0.048395408149559	0.441381132994908	−0.004577491443046	7.916782416380341	1.3582×10^{-10}
−0.048418759296854	0.441373293465484	−0.008091926987383	7.918495188373015	1.5487×10^{-10}
−0.048444823927816	0.441364658695038	−0.010736693375612	7.920403622878176	1.6372×10^{-10}
−0.048528473480437	0.441338751514823	−0.016600395053161	7.926497210705373	2.1689×10^{-10}
−0.048702054462494	0.441294227392042	−0.024699090847178	7.938981691301708	4.2225×10^{-10}
−0.048952201637010	0.441252105146249	−0.033085957123197	7.956570663474853	5.7934×10^{-11}
−0.049380482668647	0.441238793668396	−0.043871878787133	7.985516460694701	6.514×10^{-11}
−0.050120037308152	0.441375277079063	−0.057734089638779	8.031900071238120	8.2958×10^{-11}
−0.051434327434864	0.442023406792104	−0.075336525276702	8.103355935933784	1.4262×10^{-10}
−0.054119094467763	0.444413640950288	−0.098149548390364	8.211821133574361	1.7983×10^{-10}

Table 6 Data for the proofs of the axial periodic orbits.

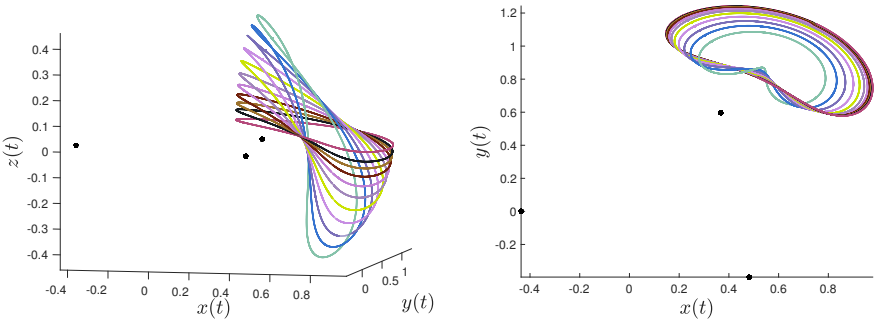

Fig. 11 (**left**) Pancake family at the mass ratio $m_1 = 0.5$, $m_2 = 0.3$ and $m_3 = 0.2$. The periods of the periodic orbits vary from 4.5763 to 4.6106. (**right**) The projection of the same family in the $x - y$ plane.

x_0	y_0	z_0	T	r
0.212455213011797	1.182772864536366	0.036991455440148	4.576291688225719	5.0779×10^{-11}
0.214437292187137	1.180184965758249	0.071075567530617	4.576794724833134	5.0393×10^{-11}
0.216607135129106	1.177364714138509	0.094910094846725	4.577349740417235	4.8827×10^{-11}
0.220130289361272	1.172812901396223	0.123548433418731	4.578260289713129	5.1758×10^{-11}
0.225584735884784	1.165823131510027	0.156697266634631	4.579692703906730	5.6541×10^{-11}
0.233917792596010	1.155244862984607	0.194578242646016	4.581933712473146	2.5474×10^{-11}
0.245900635813063	1.140145517917039	0.235040985773960	4.585264767058336	3.1643×10^{-11}
0.261782494499508	1.120102102200940	0.274572120547345	4.589864205823196	3.4029×10^{-11}
0.281882430095956	1.094240041971860	0.310980616385583	4.595935803945371	2.4635×10^{-11}
0.303226203910973	1.065637320819820	0.339055334955731	4.602553753251315	1.0038×10^{-11}
0.329832874945133	1.027766635129443	0.363968687868029	4.610638340125636	5.9881×10^{-12}

Table 7 Data for the proofs of the axial (pancake) periodic orbits.

A Proof of Lemma 3

Since γ is a solution of the differential equation we consider the first, third, and fifth components of the vector field and have that $u_2 = \dot{u}_1$, $u_4 = \dot{u}_3$ and $u_6 = \dot{u}_5$. Moreover, considering the seventh component gives

$$\dot{u}_7 = \left(-u_1u_2 - u_3u_4 - u_5u_6 + x_1u_2 + y_1u_4 + \alpha_1\right) u_7^3,$$

and since $u_7 > 0$ we divide by u_7^3 and rewrite this as

$$\begin{aligned}\frac{1}{u_7^3}\frac{d}{dt}u_7 &= -(u_1-x_1)u_2 - (u_3-y_1)u_4 - u_5u_6 + \alpha_1\\ &= -(u_1-x_1)u_1' - (u_3-y_1)u_3' - u_5u_5' + \alpha_1\\ &= -\frac{1}{2}\frac{d}{dt}(u_1-x_1)^2 - \frac{1}{2}\frac{d}{dt}(u_2-y_1)^2 - \frac{1}{2}\frac{d}{dt}(u_3)^2 + \alpha_1\\ &= -\frac{1}{2}\frac{d}{dt}\left((u_1-x_1)^2 + (u_2-y_1)^2 + u_3^2\right) + \alpha_1,\end{aligned}$$

or

$$\frac{d}{dt}G_1(t) = \frac{d}{dt}F_1(t) + \alpha_1, \tag{15}$$

where

$$F_1(t) \stackrel{\text{def}}{=} -\frac{1}{2}\left((u_1(t)-x_1)^2 + (u_3(t)-y_1)^2 + (u_1(t)-x_1)^2\right),$$

and

$$G_1(t) \stackrel{\text{def}}{=} -\frac{1}{2u_7(t)^2},$$

are both periodic functions. Taking the average of Equation (15) over the interval $[0,T]$ leads to

$$0 = \frac{1}{T}\int_0^T \alpha_1\,dt = \alpha_1,$$

as the derivatives of F_1 and G_1 (indeed the derivatives of any periodic function) have average zero. Since $T > 0$ we conclude that $\alpha_1 = 0$ as desired. Nearly identical arguments, applied to the eighth and ninth component equations, show that $\alpha_2 = \alpha_3 = 0$.

Now define

$$\hat{u}(t) \stackrel{\text{def}}{=} \frac{1}{\sqrt{(u_1(t)-x_1)^2 + (u_3(t)-y_1)^2 + u_5(t)^2}},$$

and note that

$$\begin{aligned}\frac{d}{dt}\hat{u}(t) &= -\frac{\frac{d}{dt}(u_1(t)-x_1)^2 + (u_3(t)-y_1)^2 + u_5(t)^2}{2\left(\sqrt{(u_1(t)-x_1)^2 + (u_3(t)-y_1)^2 + u_5(t)^2}\right)^3}\\ &= -\hat{u}^3\left((u_1-x_1)u_2 + (u_3-y_1)u_4 + u_5u_6\right)\\ &= -\hat{u}^3u_1u_2 - \hat{u}^3u_3u_4 - \hat{u}^3u_5u_6 + \hat{u}^3x_1u_2 + \hat{u}^3y_1u_4.\end{aligned}$$

Then we see that $u_7(t)$ and $\hat{u}(t)$ satisfy the same differential equation with the same initial condition. By existence and uniqueness for ODEs we have that $u_7(t) = \hat{u}(t)$, i.e.

$$u_7(t) = \frac{1}{\sqrt{(u_1(t)-x_1)^2 + (u_3(t)-y_1)^2 + u_5(t)^2}}. \tag{16}$$

for all $t \in [0,T]$. Similarly

$$u_8(t) = \frac{1}{\sqrt{(u_1(t)-x_2)^2 + (u_3(t)-y_2)^2 + u_5(t)^2}}. \tag{17}$$

and

$$u_9(t) = \frac{1}{\sqrt{(u_1(t)-x_3)^2 + (u_3(t)-y_3)^2 + u_5(t)^2}}. \tag{18}$$

for all $t \in [0,T]$.

The argument that $\beta = 0$ is similar to the above but different enough that we include it for the sake of completeness. Inspired by the energy functional for the circular restricted four body problem we define the function

$$H(u) = -(u_2^2 + u_4^2 + u_6^2) + u_1^2 + u_3^2 + 2\left(m_1u_7 + m_2u_8 + m_3u_9\right),$$

and observe that $H(\gamma(t))$ is a periodic function. We have that

$$\nabla H = \begin{pmatrix} 2u_1 \\ -2u_2 \\ 2u_3 \\ -2u_4 \\ 0 \\ -2u_6 \\ 2m_1 \\ 2m_2 \\ 2m_3 \end{pmatrix}.$$

Since we have already established that $\alpha_1 = \alpha_2 = \alpha_3 = 0$ we have that

$$\begin{aligned}
\langle \nabla H, g\rangle &= \left\langle \begin{pmatrix} 2u_1 \\ -2u_2 \\ 2u_3 \\ -2u_4 \\ 0 \\ -2u_6 \\ 2m_1 \\ 2m_2 \\ 2m_3 \end{pmatrix} \begin{pmatrix} u_2 \\ 2u_4 + u_1 - m_1u_1u_7^3 - m_2u_1u_8^3 - m_3u_1u_9^3 + m_1x_1u_7^3 + m_2x_2u_8^3 + m_3x_3u_9^3 + \beta u_2 \\ u_4 \\ -2u_2 + u_3 - m_1u_3u_7^3 - m_2u_3u_8^3 - m_3u_3u_9^3 + m_1y_1u_7^3 + m_2y_2u_8^3 + m_3y_3u_9^3 \\ u_6 \\ -m_1u_5u_7^3 - m_2u_5u_8^3 - m_3u_5u_9^3 + m_1z_1u_7^3 + m_2z_2u_8^3 + m_3z_3u_9^3 \\ -u_1u_2u_7^3 - u_3u_4u_7^3 - u_5u_6u_7^3 + x_1u_2u_7^3 + y_1u_4u_7^3 + z_1u_6u_7^3 \\ -u_1u_2u_8^3 - u_3u_4u_8^3 - u_5u_6u_8^3 + x_2u_2u_8^3 + y_2u_4u_8^3 + z_2u_6u_8^3 \\ -u_1u_2u_9^3 - u_3u_4u_9^3 - u_5u_6u_9^3 + x_3u_2u_9^3 + y_3u_4u_9^3 + z_3u_6u_9^3 \end{pmatrix} \right\rangle \\
&= 2u_1u_2 - 2u_2(2u_4 + u_1 - m_1u_1u_7^3 - m_2u_1u_8^3 - m_3u_1u_9^3 + m_1x_1u_7^3 + m_2x_2u_8^3 + m_3x_3u_9^3) - 2\beta u_2^2 \\
&\quad + 2u_3u_4 - 2u_4(-2u_2 + u_3 - m_1u_3u_7^3 - m_2u_3u_8^3 - m_3u_3u_9^3 + m_1y_1u_7^3 + m_2y_2u_8^3 + m_3y_3u_9^3) \\
&\quad - 2u_6(-m_1u_5u_7^3 - m_2u_5u_8^3 - m_3u_5u_9^3 + m_1z_1u_7^3 + m_2z_2u_8^3 + m_3z_3u_9^3) \\
&\quad + 2m_1(-u_1u_2u_7^3 - u_3u_4u_7^3 - u_5u_6u_7^3 + x_1u_2u_7^3 + y_1u_4u_7^3 + z_1u_6u_7^3) \\
&\quad + 2m_2(-u_1u_2u_8^3 - u_3u_4u_8^3 - u_5u_6u_8^3 + x_2u_2u_8^3 + y_2u_4u_8^3 + z_2u_6u_8^3) \\
&\quad + 2m_3(-u_1u_2u_9^3 - u_3u_4u_9^3 - u_5u_6u_9^3 + x_3u_2u_9^3 + y_3u_4u_9^3 + z_3u_6u_9^3) \\
&= 2u_1u_2 - 4u_2u_4 - 2u_2u_1 + 2m_1u_2u_1u_7^3 + 2m_2u_2u_1u_8^3 + 2m_3u_2u_1u_9^3 \\
&\quad - 2m_1u_2x_1u_7^3 - 2m_2u_2x_2u_8^3 - 2m_3u_2x_3u_9^3 - 2\beta u_2^2 \\
&\quad + 2u_3u_4 + 4u_2u_4 - 2u_3u_4 + 2m_1u_3u_4u_7^3 + 2m_2u_3u_4u_8^3 + 2m_3u_3u_4u_9^3 \\
&\quad - 2m_1y_1u_4u_7^3 - 2m_2y_2u_4u_8^3 - 2m_3y_3u_4u_9^3 \\
&\quad + 2m_1u_5u_6u_7^3 + 2m_2u_5u_6u_8^3 + 2m_3u_5u_6u_9^3 - 2m_1z_1u_6u_7^3 - 2m_2z_2u_6u_8^3 - 2m_3z_3u_6u_9^3 \\
&\quad - 2m_1u_1u_2u_7^3 - 2m_1u_3u_4u_7^3 - 2m_1u_5u_6u_7^3 + 2m_1x_1u_2u_7^3 + 2m_1y_1u_4u_7^3 + 2m_1z_1u_6u_7^3 \\
&\quad - 2m_2u_1u_2u_8^3 - 2m_2u_3u_4u_8^3 - 2m_2u_5u_6u_8^3 + 2m_2x_2u_2u_8^3 + 2m_2y_2u_4u_8^3 + 2m_2z_2u_6u_8^3 \\
&\quad - 2m_3u_1u_2u_9^3 - 2m_3u_3u_4u_9^3 - 2m_3u_5u_6u_9^3 + 2m_3x_3u_2u_9^3 + 2m_3y_3u_4u_9^3 + 2m_3z_3u_6u_9^3. \\
&= -2\beta u_2^2.
\end{aligned}$$

Then we note that $H(\gamma(t))$ is a periodic function and that the above computation gives

$$\begin{aligned}
\frac{d}{dt}H(t) &= \nabla H(\gamma(t))\gamma'(t) \\
&= \nabla H(\gamma(t))g(\gamma(t)) \\
&= -2\beta u_2^2(t).
\end{aligned}$$

Taking the average, and exploiting that the average of the derivative of a periodic function is zero gives

$$0 = \frac{1}{T}\int_0^T \frac{d}{dt}H(t)\,dt = -\frac{2\beta}{T}\int_0^T u_2(t)^2\,dt.$$

Since $T > 0$ and $u_2(t)^2$ does not change sign it follows that $\beta = 0$.

Finally we recall Equations (16), (17), and (18) as well as the fact that $\beta = 0$ and have that

$$\begin{aligned}
\dot{u}_2 &= 2u_4 + u_1 - m_1 u_1 u_7^3 - m_2 u_1 u_8^3 - m_3 u_1 u_9^3 + m_1 x_1 u_7^3 + m_2 x_2 u_8^3 + m_3 x_3 u_9^3 \\
&= 2u_4 + u_1 - m_1(u_1 - x_1)u_7^3 - m_2(u_1 - x_2)u_8^3 - m_3(u_1 - x_3)u_9^3 \\
&= 2u_4 + u_1 - \frac{m_1(u_1 - x_1)}{((u_1(t) - x_1)^2 + (u_3(t) - y_1)^2 + u_5(t)^2)^{3/2}} \\
&\quad - \frac{m_2(u_1 - x_2)}{((u_1(t) - x_2)^2 + (u_3(t) - y_2)^2 + u_5(t)^2)^{3/2}} \\
&\quad - \frac{m_3(u_1 - x_3)}{((u_1(t) - x_3)^2 + (u_3(t) - y_3)^2 + u_5(t)^2)^{3/2}} \\
&= 2u_4 + \Omega_x
\end{aligned}$$

A similar computation shows that

$$\dot{u}_4 = -2u_2 + \Omega_y,$$

and that

$$\dot{u}_6 = \Omega_z.$$

Then $\hat{\gamma}(t) \stackrel{\text{def}}{=} (u_1(t), u_2(t), u_3(t), u_4(t), u_5(t), u_6(t))$ is a periodic solution of the circular restricted four body problem as desired.

References

1. E. Strömgren. Connaissance actuelle des orbites dans le probleme des trois corps. *Bull. Astronom.*, 9(2):87–130, 1933.
2. M. Hénon. Exploration numérique du probléme restreint i. masses égales, orbites périodiques. *Ann. Astrophysics*, 28:499–511, 1965.
3. M. Hénon. Exploration numérique du probléme restreint ii. masses égales, stabilité des orbites périodiques. *Ann. Astrophysics*, 28:992–1007, 1965.
4. R. A. Broucke. Periodic orbits in the restricted three–body problem with earth-moon masses. *Technical Report, JPL*, 1968.
5. Jürgen Moser. *Stable and random motions in dynamical systems*. Princeton Landmarks in Mathematics. Princeton University Press, Princeton, NJ, 2001. With special emphasis on celestial mechanics, Reprint of the 1973 original, With a foreword by Philip J. Holmes.
6. Victor Szebehely. *Theory of Orbits: the restricted problem of three bodies*. Academic Press Inc., 1967.
7. Kenneth R. Meyer, Glen R. Hall, and Dan Offin. *Introduction to Hamiltonian dynamical systems and the N-body problem*, volume 90 of *Applied Mathematical Sciences*. Springer, New York, second edition, 2009.
8. Edward Belbruno. *Fly me to the moon*. Princeton University Press, Princeton, NJ, 2007. An insider's guide to the new science of space travel, With a foreword by Neil deGrasse Tyson.
9. Alain Chenciner. Poincaré and the three-body problem. In *Henri Poincaré, 1912–2012*, volume 67 of *Prog. Math. Phys.*, pages 51–149. Birkhäuser/Springer, Basel, 2015.
10. Farquhar R.W. *The Control and Use of Libration-Point Satellites.* PhD thesis, Stanford University. Stanford, California., 1968.
11. D. Folta and M. Beckman. Libration orbit mission design: Applications of numerical and dynamical methods. In *Libration Point Orbits and Applications, Girona, Spain*, June 2002.
12. R Schwarz, R Dvorak, A Suli, and B Erdi. Survey of the stability region of hypothetical habitable trojan planets. *Astronomy & Astrophysics.*, page 474, 2007.
13. P. Pedersen. Librationspunkte im restringierten vierkörperproblem. *Dan. Mat. Fys. Medd.*, 21(6), 1944.
14. P. Pedersen. Stabilitätsuntersuchungen im restringierten vierkörperproblem. *Dan. Mat. Fys. Medd.*, 26(16), 1952.

15. Carlos Simó. Relative equilibrium solutions in the four-body problem. *Celestial Mech.*, 18(2):165–184, 1978.
16. Martha Álvarez-Ramírez and Claudio Vidal. Dynamical aspects of an equilateral restricted four-body problem. *Math. Probl. Eng.*, pages Art. ID 181360, 23, 2009.
17. Eduardo S. G. Leandro. On the central configurations of the planar restricted four-body problem. *J. Differential Equations*, 226(1):323–351, 2006.
18. Jean F. Barros and Eduardo S. G. Leandro. The set of degenerate central configurations in the planar restricted four-body problem. *SIAM J. Math. Anal.*, 43(2):634–661, 2011.
19. Jean F. Barros and Eduardo S. G. Leandro. Bifurcations and enumeration of classes of relative equilibria in the planar restricted four-body problem. *SIAM J. Math. Anal.*, 46(2):1185–1203, 2014.
20. Jaime Burgos-García. Families of periodic orbits in the planar Hill's four-body problem. *Astrophys. Space Sci.*, 361(11):Paper No. 353, 21, 2016.
21. Jaime Burgos-Garcia and Abimael Bengochea. Horseshoe orbits in the restricted four-body problem. *Astrophys. Space Sci.*, 362(11):Paper No. 212, 14, 2017.
22. Jaime Burgos-García and Joaquín Delgado. Periodic orbits in the restricted four–body problem with two equal masses. *Astrophysics and Space Sciences*, 345(2):247–263, 2013.
23. K. E. Papadakis. Families of asymmetric periodic solutions in the restricted four-body problem. *Astrophys. Space Sci.*, 361(12):Paper No. 377, 15, 2016.
24. A. N. Baltagiannis and K. E. Papadakis. Families of periodic orbits in the restricted four-body problems. *Astrophysical Space Science*, 366:357–367, 2011.
25. K. E. Papadakis. Families of three-dimensional periodic solutions in the circular restricted four-body problem. *Astrophys. Space Sci.*, 361(4):Paper No. 129, 14, 2016.
26. Allan Hungria, Jean-Philippe Lessard, and Jason D. Mireles-James. Rigorous numerics for analytic solutions of differential equations: the radii polynomial approach. *Math. Comp.*, 85(299):1427–1459, 2016.
27. Jean-Philippe Lessard, J. D. Mireles James, and Julian Ransford. Automatic differentiation for Fourier series and the radii polynomial approach. *Phys. D*, 334:174–186, 2016.
28. J. B. Van den Berg and Ray Sheombarsing. Rigorous numerics for odes using chebyshev series and domain decomposition. *(Submitted)*, pages 1–32, 2016.
29. J.P. Lessard. Computing discrete convolutions with verified accuracy via banach algebras and the fft. *Applications of Mathematics*, 2018.
30. J. Burgos-García. *Órbitas periodicas en el problema restringido de cuatro cuerpos.* PhD thesis, UAM-I, 2013.
31. Ariadna Farrés and Àngel Jorba. On the high order approximation of the centre manifold for ODEs. *Discrete Contin. Dyn. Syst. Ser. B*, 14(3):977–1000, 2010.
32. H. B. Keller. *Lectures on numerical methods in bifurcation problems*, volume 79 of *Tata Institute of Fundamental Research Lectures on Mathematics and Physics*. Published for the Tata Institute of Fundamental Research, Bombay, 1987. With notes by A. K. Nandakumaran and Mythily Ramaswamy.
33. F. J. Muñoz Almaraz, E. Freire, J. Galán, E. Doedel, and A. Vanderbauwhede. Continuation of periodic orbits in conservative and Hamiltonian systems. *Phys. D*, 181(1-2):1–38, 2003.
34. M. Hénon. Vertical stability of periodic orbits in the restricted problem. i. equal masses. *Astronomy and Astrophysics*, 28:415–426, 1973.
35. Warwick Tucker. *Validated numerics.* Princeton University Press, Princeton, NJ, 2011. A short introduction to rigorous computations.
36. J.-P. Eckmann, H. Koch, and P. Wittwer. A computer-assisted proof of universality for area-preserving maps. *Mem. Amer. Math. Soc.*, 47(289):vi+122, 1984.
37. Jan Bouwe van den Berg and Jean-Philippe Lessard. Rigorous numerics in dynamics. *Notices of the American Mathematical Society*, 62(9):1057–1061, 2015.
38. Hans Koch, Alain Schenkel, and Peter Wittwer. Computer-assisted proofs in analysis and programming in logic: a case study. *SIAM Rev.*, 38(4):565–604, 1996.
39. Maciej J. Capiński and Pablo Roldán. Existence of a center manifold in a practical domain around L_1 in the restricted three-body problem. *SIAM J. Appl. Dyn. Syst.*, 11(1):285–318, 2012.
40. Maciej J. Capiński and Anna Wasieczko-Zajac. Geometric proof of strong stable/unstable manifolds with application to the restricted three body problem. *Topol. Methods Nonlinear Anal.*, 46(1):363–399, 2015.
41. Shane Kepley and J. D. Mireles James. Chaotic motions in the restricted four body problem via devaney's saddle-focus homoclinic tangle theorem. *(Submitted)* `https://arxiv.org/abs/1711.06932`, pages 1–67, 2017.

42. Gianni Arioli. Branches of periodic orbits for the planar restricted 3-body problem. *Discrete Contin. Dyn. Syst.*, 11(4):745–755, 2004.
43. Tomasz Kapela and Piotr Zgliczyński. The existence of simple choreographies for the N-body problem—a computer-assisted proof. *Nonlinearity*, 16(6):1899–1918, 2003.
44. Irmina Walawska and Daniel Wilczak. Continuation and bifurcations of halo orbits in the circular restricted three body problme. *(In preperation)*, 2018.
45. Alessandra Celletti and Luigi Chierchia. On the stability of realistic three-body problems. *Comm. Math. Phys.*, 186(2):413–449, 1997.
46. Alessandra Celletti and Luigi Chierchia. KAM stability and celestial mechanics. *Mem. Amer. Math. Soc.*, 187(878):viii+134, 2007.
47. Alessandra Celletti and Luigi Chierchia. Rigorous estimates for a computer-assisted KAM theory. *J. Math. Phys.*, 28(9):2078–2086, 1987.
48. Alessandra Celletti, Corrado Falcolini, and Anna Porzio. Rigorous numerical stability estimates for the existence of KAM tori in a forced pendulum. *Ann. Inst. H. Poincaré Phys. Théor.*, 47(1):85–111, 1987.
49. R. de la Llave and David Rana. Accurate strategies for small divisor problems. *Bull. Amer. Math. Soc. (N.S.)*, 22(1):85–90, 1990.
50. Alessandra Celletti and Luigi Chierchia. A computer-assisted approach to small-divisors problems arising in Hamiltonian mechanics. In *Computer aided proofs in analysis (Cincinnati, OH, 1989)*, volume 28 of *IMA Vol. Math. Appl.*, pages 43–51. Springer, New York, 1991.
51. À. Haro and R. de la Llave. A parameterization method for the computation of invariant tori and their whiskers in quasi-periodic maps: numerical algorithms. *Discrete Contin. Dyn. Syst. Ser. B*, 6(6):1261–1300 (electronic), 2006.
52. Tomasz Kapela and Carles Simó. Rigorous kam results around arbitrary periodic orbits for hamiltonian systems. *(Submitted))*.
53. Joseph Galante and Vadim Kaloshin. Destruction of invariant curves in the restricted circular planar three-body problem by using comparison of action. *Duke Math. J.*, 159(2):275–327, 2011.
54. John C. Urschel and Joseph R. Galante. Instabilities in the Sun-Jupiter-asteroid three body problem. *Celestial Mech. Dynam. Astronom.*, 115(3):233–259, 2013.
55. Gianni Arioli. Periodic orbits, symbolic dynamics and topological entropy for the restricted 3-body problem. *Comm. Math. Phys.*, 231(1):1–24, 2002.
56. Daniel Wilczak and Piotr Zgliczynski. Heteroclinic connections between periodic orbits in planar restricted circular three-body problem—a computer assisted proof. *Comm. Math. Phys.*, 234(1):37–75, 2003.
57. Daniel Wilczak and Piotr Zgliczyński. Heteroclinic connections between periodic orbits in planar restricted circular three body problem. II. *Comm. Math. Phys.*, 259(3):561–576, 2005.
58. Maciej J. Capiński. Computer assisted existence proofs of Lyapunov orbits at L_2 and transversal intersections of invariant manifolds in the Jupiter-Sun PCR3BP. *SIAM J. Appl. Dyn. Syst.*, 11(4):1723–1753, 2012.
59. Marcio Gameiro and Jean-Philippe Lessard. A Posteriori Verification of Invariant Objects of Evolution Equations: Periodic Orbits in the Kuramoto–Sivashinsky PDE. *SIAM J. Appl. Dyn. Syst.*, 16(1):687–728, 2017.
60. Sarah Day, Jean-Philippe Lessard, and Konstantin Mischaikow. Validated continuation for equilibria of PDEs. *SIAM J. Numer. Anal.*, 45(4):1398–1424 (electronic), 2007.
61. Nobito Yamamoto. A numerical verification method for solutions of boundary value problems with local uniqueness by Banach's fixed-point theorem. *SIAM J. Numer. Anal.*, 35(5):2004–2013 (electronic), 1998.
62. Gianni Arioli and Hans Koch. Non-symmetric low-index solutions for a symmetric boundary value problem. *J. Differential Equations*, 252(1):448–458, 2012.
63. J. F. Steffensen. On the differential equations of Hill in the theory of the motion of the moon. *Acta Math.*, 93:169–177, 1955.
64. Eugene Rabe. Determination and survey of periodic Trojan orbits in the restricted problem of three bodies. *Astronom. J.*, 66:500–513, 1961.
65. André Drprit and J.F. Price. The computation of characterist exponents in the palnar restricted problem of three bodies. *Boeing Scientific Research Labortories, Mathematics Research Laboratory*, Mathematical Note(Number 415):1–84, 1965.
66. Àngel Jorba and Maorong Zou. A software package for the numerical integration of ODEs by means of high-order Taylor methods. *Experiment. Math.*, 14(1):99–117, 2005.

67. Donald E. Knuth. *The art of computer programming. Vol. 2.* Addison-Wesley Publishing Co., Reading, Mass., second edition, 1981. Seminumerical algorithms, Addison-Wesley Series in Computer Science and Information Processing.
68. Àlex Haro, Marta Canadell, Jordi-Lluí s Figueras, Alejandro Luque, and Josep-Maria Mondelo. *The parameterization method for invariant manifolds*, volume 195 of *Applied Mathematical Sciences*. Springer, [Cham], 2016. From rigorous results to effective computations.
69. Jan Bouwe van den Berg, Maxime Breden, Jean-Philippe Lessard, and Maxime Murray. Continuation of homoclinic orbits in the suspension bridge equation: a computer-assisted proof. *J. Differential Equations*, 264(5):3086–3130, 2018.
70. Jacques-Alexandre Sepulchre and Robert S. MacKay. Localized oscillations in conservative or dissipative networks of weakly coupled autonomous oscillators. *Nonlinearity*, 10(3):679–713, 1997.
71. F. J. Muñoz Almaraz, J. Galán, and E. Freire. Numerical continuation of periodic orbits in symmetric Hamiltonian systems. In *International Conference on Differential Equations, Vol. 1, 2 (Berlin, 1999)*, pages 919–921. World Sci. Publ., River Edge, NJ, 2000.
72. S.M. Rump. INTLAB - INTerval LABoratory. In Tibor Csendes, editor, *Developments in Reliable Computing*, pages 77–104. Kluwer Academic Publishers, Dordrecht, 1999. http://www.ti3.tu-harburg.de/rump/.
73. E. J. Doedel, V. A. Romanov, R. C. Paffenroth, H. B. Keller, D. J. Dichmann, J. Galán-Vioque, and A. Vanderbauwhede. Elemental periodic orbits associated with the libration points in the circular restricted 3-body problem. *Internat. J. Bifur. Chaos Appl. Sci. Engrg.*, 17(8):2625–2677, 2007.
74. R. C. Calleja, E. J. Doedel, A. R. Humphries, A. Lemus-Rodrí guez, and E. B. Oldeman. Boundary-value problem formulations for computing invariant manifolds and connecting orbits in the circular restricted three body problem. *Celestial Mech. Dynam. Astronom.*, 114(1-2):77–106, 2012.